Preprint
UCRL-JRNL-205916

Present and Future Surface Climate in the Western U.S. as simulated by 15 Global Climate Models

J. Coquard, P.B. Duffy, and K. E. Taylor Lawrence Livermore National Laboratory J. P. Iorio, Stanford University

This article was submitted to Climate Dynamics

U.S. Department of Energy
Lawrence Livermore National Laboratory

August 2004

DISCLAIMER

Present and Future Surface Climate in the Western U.S. as simulated by 15 Global Climate Models

J. Coquard, P.B. Duffy, and K. E. Taylor
Lawrence Livermore National Laboratory

J. P. Iorio, Stanford University

Corresponding author: P.B. Duffy
pduffy@llnl.gov
Tel: (925) 422-3722
Fax: (925) 422-6388

Abstract

We analyze results of 15 global climate simulations contributed to the Coupled Model Intercomparison Project (CMIP). Focusing on the western U.S., we consider both present climate simulations and predicted responses to increasing atmospheric CO_2.

The models vary in their ability to predict the present climate. Over the western U.S., a few models produce a seasonal cycle for spatially-averaged temperature and/or precipitation in good agreement with observational data. Other models tend to over-predict precipitation in the winter or exaggerate the amplitude of the seasonal cycle of temperature. The models also differ in their ability to reproduce the spatial patterns of temperature and precipitation in the U.S.

Considering the monthly mean precipitation responses to doubled atmospheric CO_2, averaged over the western U.S., we find some models predict increases while others predict decreases. The predicted temperature response, on the other hand, is invariably positive over this region; however, for each month, the range of values given by the different models is large compared to the mean model response.

We look for possible relationships between the models' temperature and precipitation responses to doubled CO_2 concentration and their ability to simulate some aspects of the present climate. We find that these relationships are weak, at best. The precipitation response over the western U.S. in DJF and the precipitation response over

the mid- and tropical latitudes seem to be correlated with the RMS error in simulated present-day precipitation, also calculated over the mid- and tropical latitudes. However, considering only the responses of the models with the smallest RMS errors does not provide a different estimate of the precipitation response to a doubled CO_2 concentration, because even among the most accurate models, the range of model responses is so large. For temperature, we find that models that have smaller RMS errors in present-climate temperature in the North Eastern Pacific region predict a higher temperature response in the western U.S. than the models with larger errors. A similar relation exists between the temperature response over Europe in DJF and the RMS error calculated over the Northern Atlantic.

Introduction

When information on future climate change is sought, at spatial scales not currently resolved by global climate models, "downscaling" techniques are typically used. The downscaling can be performed dynamically, using a nested regional climate model, or statistically, using empirical relationships developed from observations of the present climate. The results of both these downscaling approaches depend strongly on the large-scale driving fields obtained from the global climate model. Thus, an important component of the uncertainty in predicted regional climate changes is the range of climate changes predicted by global climate models in relevant geographical regions.

In this paper, we examine simulations of the western continental United States performed with global climate models, with the goals of assessing the predicted climate responses to increased atmospheric CO_2, as well as the inter-model variance in these predicted responses. Our focus on the western U.S. is motivated by the fact that this region may be unusually sensitive to climate change. Increases in temperature or other climate perturbations could have a large impact on local resources such as water availability. Predicting changes in climate and their consequences is therefore of great economical importance. We are also interested in the range of climate responses to

increased CO_2 over the western U.S., with the prospect of running a regional climate model over this region.

To determine the degree to which models agree, we compute the ratio of the mean response of the models to the standard deviation of their responses. This ratio is in some sense a measure of the signal to noise in predicted climate changes. We will show, for example, that the inter-model standard deviation in predicted precipitation changes in the western U.S. exceeds the model-mean predicted precipitation response; this leads to the conclusion that we cannot confidently predict even the sign of the precipitation response in this region.

As a first step, we assess the inter-model means, standard deviations, and "signal to noise ratios" in predicted climate changes under the assumption that all the models considered are equally credible. Next, we attempt to obtain more precise estimates of these quantities by considering only models that can simulate today's climate with relative accuracy. The more precise estimates could be interpreted as also being more accurate under the assumption that models that reproduce today's climate more accurately make more accurate predictions of future climate. (This assumption is implicit in the widely-accepted approach of evaluating climate models by comparing them to observations of the present climate.) If we believe that models that more accurately reproduce today's climate are inherently more credible than other models, and if these more accurate models give systematically different predicted responses to increased atmospheric CO_2 than less accurate models, we could obtain more accurate estimates of the mean and variance in predicted climate responses.

We therefore turn to searching for relationships between predicted precipitation and surface temperature responses and various measures of how well models reproduce observations of today's climate. For the most part we find no significant relationships; that is we find scant evidence that models that are relatively good at reproducing aspects of today's climate predict systematically different responses to increased atmospheric CO_2 compared to other models. We also find no evidence that models with a better ability to simulate aspects of today's climate have a narrower range of temperature or precipitation responses. Thus, in general, we do not obtain significantly different estimates of model-mean predicted responses, or of the inter-model variance in predicted

responses (which is a measure of uncertainty in the responses), by considering only models that reproduce aspects of today's climate relatively well.

Data Sources and Methods

Our analysis is based on results of 15 global coupled ocean-atmosphere general circulation models submitted to the Coupled Model Intercomparison Project, Phase 2 (CMIP2) (Table 1) [1]. The CMIP database includes coupled GCM control runs in which CO_2, solar brightness and other external climatic forcing are kept constant. Individual CMIP control runs use different values of solar "constant", ranging from 1354 to 1370 W m^{-2} and different values of CO_2 concentrations, ranging from pre-industrial values (290 ppm) to near-present climate values (345 ppm). CMIP also collected output from the same set of models in which CO_2 increases at the rate of 1% per year. For our analysis, we use both the control run output and the increasing-CO_2 simulations. For the analysis of present climate, we take results from a 20-year time window centered on the 71st year of each control simulation. To estimate the response to doubled CO_2 concentration, we subtract these results of the control simulation from results of the increasing-CO_2 simulation from the same time window. The 71st year corresponds to the time of doubling of the atmospheric CO_2 concentration. Before subtraction, the data were regridded to a common grid of 2.5 degrees by 2.5 degrees.

Model	Institution/Country	Control Run CO2 [ppmv]	Atmospheric Resolution	Ocean Resolution
GFDL_R15_a	GFDL/USA	360	R15 (4.5 x 7.5) L9	4.5 x 3.7 L12
GOALS	LASG/China	345	R15 (4.5 x 7.5) L9	4.0 x 5.0 L20
ECHAM3/LSG	ECMWF/UK	345	T21 (5.6 x 5.6) L19	4.0 x 4.0 L11
CCSR/NIES	Univ. of Tokyo/Japan	345	T21 (5.6 x 5.6) L20	2.8 x 2.8 L17
GISS2	NASA-GISSS/USA	315	4.0 x 5.0 L9	4.0 x 5.0 L13
MRI1	Meteorological Res. Inst./Japan	345	4.0 x 5.0 L15	2.0 x 2.5 L21
IPSL-CM2	IPSL/France	320	5.6 x 3.8 L15	2.0 x 2.0 L31
BMRCb	BMRC/Australia	330	R21 (3.2 x 5.6) L17	3.2 x 5.6 L12
CSIRO Mk2	CSIRO/Australia	330	R21 (3.2 x 5.6) L9	3.2 x 5.6 L21
ARPEGE/OPA2	CERFACS/France	353	T31 (3.9 x 3.9) L19	2.0 x 2.0 L31
CGCM1	CCCMA/Canada	330	T32 (3.8 x 3.8) L10	1.8 x 1.8 L29
HadCM3	UKMO/UK	289.6	2.5 x 3.75 L19	1.25 x 1.25 L20
HadCM2	UKMO/UK	322.6	2.5 x 3.75 L19	2.5 x 3.75 L20
CSM1.0	NCAR/USA	355	T42 (2.8 x 2.8)	2.0 x 2.4

			L18	L45
DOE PCM	NCAR	355	T42 (2.8 x 2.8) L18	0.67 x 0.67 L32

Table 1: List of the 15 CMIP models with their control run CO_2 concentration, atmospheric resolution and ocean resolution. Models are listed in order of number of horizontal grid cells in the atmospheric component.

In order to assess the ability of the models to simulate aspects of the present climate, we compare the simulated precipitation to observational data and the simulated temperatures to reanalysis data. The observational data for precipitation are provided by the Climate Prediction Center (CPC) Merged Analysis of Precipitation ("CMAP") [2]; we consider the data from 1979 through 1997. We obtain the reanalysis data for temperatures from the years 1979 to 1997 of the National Centers for Environmental Prediction Reanalysis-2 Project (NCEP2) [3]. We also consider the temperature reanalysis data from 1979 to 1993 provided by the European Center for Medium-Range Weather Forecast ERA15 Project [4]. Although the results we get from the comparison of the model temperatures to the two reanalysis temperatures are slightly different, the main conclusions are the same, and we choose to present only the results of the study performed with the NCEP2 reanalysis data.

For the purpose of analyzing the simulations of present climate and the response to doubled CO_2 concentration predicted by the 15 CMIP models, we consider two geographical regions: The first region is located between latitudes 31 degrees N and 48 degrees N and longitudes 114 degrees W and 125 degrees W; it includes most of the western United States as well as a small portion of the Pacific Ocean. Within this region we compare the seasonal cycles of spatially-averaged simulated temperature and precipitation to observations. We also compute responses to doubled CO_2 concentration over this region. This region is too small, however, to meaningfully evaluate the ability of coarse-resolution models to simulate spatial patterns of climatic quantities. We therefore consider a second, larger region, which extends approximately from latitudes 24 degrees N to 51 degrees N and from longitudes 62 degrees W to 130 degrees W. This region

includes all the continental United States and part of Mexico. In this region we compare simulated to observed spatial patterns of temperature and precipitation.

Previous Studies

Previous studies reported temperature and precipitation responses to increased atmospheric CO_2 in some states in the western U.S., as predicted either by general circulation models (GCMs) or by a nested regional climate model (RCM) driven by a GCM. Although our goal in this paper is different from the goal of these studies, we examine if the results are consistent with each other.

Giorgi *et al*. (1994) discuss present-climate and doubled CO_2 simulations of the continental United States, using the MM4 RCM nested within the NCAR CCM. For near-surface temperatures, they find that both models have spatially-averaged monthly mean temperature responses to doubled CO_2 concentration ranging from about 3K to 5K over the Southwestern U.S. and from about 2K to 6K over the Northwestern U.S. For precipitation, the spatially-averaged monthly mean response to doubled CO_2 is almost always predicted to be positive over the Northwestern U.S., while it is almost always predicted to be negative from April to October over the Southwestern U.S. and positive the rest of the year.

Kim *et al*. (2002) simulated present and increased-CO_2 climates in Western U.S. using an RCM nested within two scenarios from UKMO's HadCM2 GCM. They find that for every season, temperature signals prediscted by the GCM and RCM are in ranges 3 - 4K and 3 – 5 K, respectively, in most of the western U.S. As far as precipitation is concerned, they find that the GCM projects large winter and fall precipitation increases in the western U.S. and small increases or even decreases in the spring and summer. The downscaled spatially-averaged precipitation signal shows characteristics similar to the GCM signal.

Leung and Ghan (1999) simulated an increased-CO_2 climate in Washington, Oregon, Idaho and Montana, using the PNNL RCM nested within the NCAR CCM3 GCM The GCM was forced with observed SSTs to simulate the present climate, and with SSTs from a simulation with the GFDL coupled model to simulate an increased GHG climate.

They find that for surface temperature, both the GCM and RCM "show warming between 0 degree C and 4.5 degrees C throughout all seasons and over" all four states. In all four regions, the precipitation signals fluctuate from high positive values in some months to high negative values in other months. The RCM and the GCM both predict negative precipitation signals over all the states in a few months.

Snyder *et al.* (2002) used the RegCM2 RCM nested within the CCM3 GCM coupled to a slab ocean model to generate ensembles of climate scenarios under atmospheric conditions of 280 and 560 ppm CO_2 for a domain centered over California. They found that although monthly results are noisy, the temperature response is positive over the whole region, every month. The precipitation response however, is negative in some months in certain regions.

The areas considered in these four studies do not perfectly match with the western U.S. region considered in our own study; the results that these studies report were partially obtained from RCMs, as opposed to our study which only analyzes GCM results, and the experimental conditions in these studies are all different from the conditions in which the data we analyze were obtained. However, since they all report the climate response to increased CO_2 over the western U.S., we can still look at the consistency of our results with their general conclusions.

Despite the differences between the predicted responses to increased atmospheric CO_2 over the western U.S. of the different studies, overall, the temperature response is found to be significantly positive over the whole region and in every season. The precipitation response is usually predicted to be large and positive in the winter, while in the summer it is usually smaller, negative at least over part of the domain and not significant. As we will see later, these general results are consistent with our findings, which are that the 15-model mean temperature response is significantly positive over the western U.S. We also find that the model-mean precipitation response is small and negative in summer / fall, larger and positive in winter, but never significantly different from zero.

Pan *et al.* (2001) examined simulations of precipitation in the continental U.S. performed with two different RCMs driven by reanalysis, and by simulations with the HadCAM2 GCM of the present climate and an increased greenhouse gas climate. They

quantified precipitation biases due to errors in the RCMs, errors in the GCM boundary conditions, and differences between the two RCMs, in different seasons. They found that many of these biases are largest in summer, possibly due to increased reliance on parameterizations in that season. They also found that, in summer, precipitation responses to increased greenhouse gases are everywhere less than precipitation biases, again possibly due to a predominance of convective precipitation in this season.

Kittel *et al*. (1998) examined regional biases and transient doubled CO_2 sensitivities of nine coupled atmosphere-ocean models: the CSIRO MK2O, GFDL_R15_A, MPI-m, MPI-x, MRI1, NCAR-q, NCAR-r, HADCM2-s and HADCM2-t models. The focused on seven continental regions: Central North America, Southern Europe, Northern Europe, the Sahel, Southern Asia, Eastern Asia, and Australia. The models showed surface warming in all regions, with slightly stronger temperature sensitivity in winter. Precipitation changes were mostly in the range of – 20 % to 20 % of controls. "Across all models and regions, there was a slight trend towards increasing precipitation, with larger responses in winter (average change = 7 ± 20 %) than in summer (2 ± 11 %)."

Although none of the regions considered in this study correspond to the western U.S., the fact that over all these regions, the models all predict a significantly positive temperature response both in DJF and JJA, and the fact that over five regions out of seven, the range of model precipitation responses includes zero both in DJF and JJA are consistent with our results. Despite some large differences between their responses, the models seem to always predict a positive temperature response to increased CO_2. In contrast, over many regions, models don't agree on the sign of the precipitation response to increased CO_2 concentration.

Covey *et al*. (2003) report results of control simulations and 1% per year increasing CO_2 simulations performed by 18 CMIP models. They calculate the annual mean precipitation and temperature responses to increased CO_2 concentration by subtracting the first 20-year means of the 80-year perturbed simulations from the last 20-year means of the same simulations. They calculate the all-model mean precipitation and temperature responses and normalize them by the respective standard deviation over the 18 models. They find that everywhere over the continental U.S., the normalized annual mean temperature response averaged over the 18 models is greater than one, while the

normalized annual mean precipitation response has an absolute value less than one. This result is consistent with what we find for the DJF and JJA precipitation and temperature responses over the U.S.

Results

1. Simulation of present Climate

1.1 Seasonal cycles of precipitation and temperature over the western U.S.

We are interested in how accurately the different CMIP models simulate precipitation and near-surface temperature over the United States. We first focus on the western U.S., where the seasonal cycles are strong. For each model, we compare the seasonal cycle of simulated climatological precipitation and near-surface temperature, spatially averaged over the western U.S., to the comparable values obtained respectively from observations and reanalysis.

All the models overpredict winter precipitation (Figure 1); in some of the models (BMRCb, GFDL_R15_a, GOALS, IPSL-CM2, HadCM2, and HadCM3), precipitation rates are more than 50% above the observations. Some models tend to overpredict precipitation over most of the year except in July, August and September. For most of these models, the simulated precipitation in autumn, winter and spring exceeds the observed precipitation by 0.3 mm/day to 1 mm/day, while in the summer, the simulated precipitation generally matches the observations. In three models (CCSR/NIES, ECHAM3/LSG and MRI1), however, simulated monthly-mean precipitation is generally within 0.5 mm/day above or below observations (Fig. 1). The climatological precipitation averaged over the 15 models (Fig. 2) confirms the previous conclusions that most models overpredict precipitation in this region, especially during winter.

To gain a feel for observational uncertainties in near-surface temperatures in the region of interest, in Figure 3a we show seasonal cycles of spatially-averaged near-surface temperatures from six reanalysis or observational data sets. The different data sets differ by as much as 2 K in some months. Nonetheless, the some of the models have biases which are apparently outside the bounds of observational uncertainties. Several models (BMRCb, CCSR/NIES, ARPEGE/OPA2, IPSL-CM2 and MRI1) overestimate the near-surface temperatures in the summer by as much as 3 to 6 K (Figure 3). The same models also tend to overpredict the other seasons' temperatures but generally by no more than 3 K. Other models (GFDL_R15_a, DOE PCM, CSM1.0, GOALS, GISS2, HadCM2

and HadCM3) underestimate the temperatures in winter and spring, and except for CSM1.0, they tend to overestimate the temperatures in the summer season, generally by 1 to 3K. Thus, this second group of models overestimates the seasonal cycle in near-surface temperature in the western U.S. The GOALS model overestimates the July and August temperatures by 5K. Finally, 3 models (CGCM1, CSIRO Mk2, and ECHAM3/LSG) predict a seasonal cycle of temperature in good agreement with reanalysis. Their simulated monthly mean temperatures usually differ from the reanalysis temperatures by less than 2 K (Fig. 3).

1.2 Precipitation and temperature spatial patterns in present climate over the continental United States

In this section, we assess how well the 15 CMIP models simulate the spatial patterns of present climate temperature and precipitation over the U.S. in DJF and JJA.

Figs. 4a and 5a show, respectively, the DJF and JJA observed precipitation in the U.S., averaged over 1979 through 1997. Figs. 4b and 5b show DJF and JJA precipitation, based on 19 years of output and averaged over all 15 models. And Figs. 4c and 5c show for DJF and JJA, respectively, the difference between the all-model mean precipitation (Figs. 4b and 5b) and the observed precipitation (Figs. 4a and 5a). Finally, Figs. 4d and 5d show the difference between the all-model mean precipitation and the observed precipitation, normalized by observed interannual variability, for DJF and JJA, respectively.

The mean model simulates some of the main spatial patterns of precipitation relatively well in both DJF and JJA. However, in DJF, the models therefore overpredict precipitation in eastern Washington, eastern Oregon, Idaho, Montana, Wyoming, Utah and Nevada. The likely reason for that is that these regions are in the “rain-shadow” of mountain ranges whose maximum elevation is unrealistically low in these coarse-resolution models. In addition, mean model fails to represent the region of high precipitation over the south-eastern U.S., while in JJA in Northeastern states are too wet. In JJA, Fig. 5c shows that the wet region in the Midwest is displaced westward; they also show that over Mexico, and over the Gulf of Mexico, JJA precipitation is incorrectly

represented. Relative to observed interannual variability, errors in model-mean simulated DJF precipitation are particularly large in the Northwest (Fig. 4d); in JJA these normalized errors are generally smaller than in DJF (Fig 5d).

Figs. 6a and 7a show, respectively, the DJF and JJA temperature over the U.S. from the NCEP2 reanalysis, averaged over 1979 through 1997. Figs 6b and 7b show the corresponding simulated DJF and JJA near-surface temperatures based on 19 years of output and averaged over all 15 models. Figs. 6c and 7c show for DJF and JJA, respectively, the difference between the all-model mean near-surface temperature and the NCEP2 reanalysis temperature. And Figs. 6d and 7d show for DJF and JJA, respectively, the root mean square (RMS) difference between the model-mean simulated temperature (averaged over 19 years) and NCEP2 temperatures (for 1979 through 1997).

As for precipitation, the main spatial patterns of temperature over the U.S. in DJF and JJA are overall successfully simulated by the 15 CMIP models. In DJF, models tend to underestimate the north-south gradient in temperature. In some locations in the Western U.S., these errors exceed interannual temperature variability. In JJA, the all-model mean near-surface temperatures are too warm in most regions of the U.S. In the Western U.S., errors in the all-model mean near-surface temperatures (relative to reanalysis) greatly exceed interannual variability. Large RMS differences over certain regions where the all-model mean temperature is relatively close to reanalysis indicate a large inter-model temperature "spread" in these resgions. This is the case for example in JJA, over the north-eastern U.S. and south-eastern Canada.

To lend some sense of scale to the model errors, in Figs. 6e and 7e we show the error in all-model mean near-surface temperature (for DJF and JJA, respectively), normalized by observed interannual variability in near-surface temperature. The latter quantity here is defined to be the standard deviation over years of the seasonal-mean near-surface temperature. When normalized in this way, the all-model mean in DJF is smaller than that in JJA.

1.3 RMS errors in the simulated precipitation and temperature over the United States

In this section, we compare the different models based on the RMS errors of the simulated precipitation and temperature over the continental U.S., in DJF and JJA, with respect to observations or reanalysis.

DJF

rank	model	RMS error
1	HadCM3	0.93
2	DOE PCM	0.94
3	CSM 1.0	0.97
4	HadCM2	1.03
5	CCSR/NIES	1.12
6	GISS2	1.15
7	CSIR0 Mk2	1.15
8	ECHAM3/LSG	1.22
9	ARPEGE/OPA2	1.28
10	MRI1	1.29
11	GOALS	1.37
12	CGCM1	1.40
13	GFDL_R15_a	1.44
14	IPSL-CM2	1.66
15	BMRCb	1.70

JJA

rank	model	RMS error
1	HadCM3	0.75
2	HadCM2	O.93
3	CSIRO Mk2	1.02
4	ARPEGE/OPA2	1.06
5	GOALS	1.12
6	ECHAM3/LSG	1.19
7	CSM 1.0	1.29
8	GFDL_R15_a	1.37
9	BMRCb	1.38
10	GISS2	1.50
11	DOE PCM	1.55
12	CCSR/NIES	1.57
13	IPSL-CM2	1.75
14	MRI1	1.76
15	CGCM1	1.88

Tables 2 and 3: RMS errors of the precipitation over the U.S. in DJF and JJA respectively, calculated for each model with respect to observations

A comparison of Tables 1 through 5 suggests that there may be some relationship between horizontal spatial resolution in the AGCM component and ability to simulate precipitation and near-surface temperature. This is true of DJF precipitation and of near-surface temperature in both DJF and JJA, but not of JJA precipitation. This is consistent with the results of Duffy et al. (2003) who showed that ability to simulate precipitation in the continental U.S. is strongly resolution-dependent for DJF precipitation—which is dominated by the large-scale component—but has little resolution dependence for JJA precipitation, which is dominated by the convective component. That ability to simulate near-surface temperature should be resolution-dependent is not surprising, since the region in question has strong topographic variations.

DJF JJA

rank	model	RMS error
1	DOE PCM	1.79
2	CSM 1.0	1.85
3	HadCM3	1.90
4	CSIRO Mk2	1.92
5	GFDL_R15_a	2.15
6	ECHAM3/LSG	2.24
7	BMRCb	2.43
8	CCSR/NIES	2.62
9	HadCM2	2.96
10	CGCM1	3.07
11	MRI1	3.28
12	GISS2	3.31
13	ARPEGE/OPA2	3.38
14	GOALS	3.58
15	IPSL-CM2	3.81

rank	model	RMS error
1	HadCM3	1.34
2	CGCM1	1.58
3	CSIRO Mk2	1.61
4	HadCM2	1.85
5	CSM 1.0	1.87
6	DOE PCM	1.95
7	ARPEGE/OPA2	2.32
8	GISS2	2.40
9	GFDL_R15_a	2.53
10	ECHAM3/LSG	2.64
11	IPSL-CM2	2.80
12	CCSR/NIES	3.47
13	BMRCb	3.81
14	GOALS	4.63
15	MRI1	5.22

Tables 4 and 5: RMS errors of the temperature over the U.S. in DJF and JJA respectively, calculated for each model with respect to reanalysis

The HadCM3 model shows the third best agreement with reanalysis for temperature in DJF and has the best ability to simulate temperature in JJA and precipitation both in DJF and JJA over the U.S. The CSM 1.0 and HadCM2 models are both three times out of four among the five best models to predict present climate temperature or precipitation in DJF or JJA over the U.S.

2. Response to doubled CO_2 concentration

The seasonal cycle of spatially averaged regional temperature and precipitation responses were calculated for each model over the Western U.S. As shown by Fig. 8a, the precipitation response averaged over the 15 models is negative and very small from March to September when precipitation itself is light in this region. The relatively small inter-model standard deviation in summer precipitation shows that this is a result of small responses in individual models. In October and November, the precipitation response averaged over the models is larger, but still negative (about – 0.15 mm/day). In DJF, the model-averaged precipitation response is roughly + 0.25 mm/day, but the standard

deviation among the model responses is very large (0.75 mm/day), indicating a poor agreement of the models on the amplitude and even the sign of the regional precipitation response. Fig. 8b – in which the response is given as a percentage of the present day value – shows similar results; however, the model-averaged relative precipitation response and the associated inter-model variability are now larger in the summer / fall. The relative precipitation response averaged over the 15 models ranges from +10 % in February to -15 % in October. These two diagrams show that over the western U.S., there is a strong disagreement between the models as far as the precipitation response to doubled CO_2 is concerned. The models tend to predict a small negative response during the summer / fall when precipitation is low and a larger positive response in winter when precipitation is high, but the inter-model variability is large all year long.

Fig. 9 shows the seasonal cycle of temperature response over the western U.S., averaged over the 15 models. The model-averaged temperature response is positive in all the months; it is higher during the warm season (2.5 K – 2.8 K), from June to October than during the cold season (1.8 K – 2.4 K), from November to May. Nevertheless, the inter model variability, represented by the standard deviation over the model responses is quite significant in each month (0.5 K - 1 K), compared to the amplitude of the response itself. This indicates that the range of predicted values is quite large; however, this range is not large enough to encompass zero, and all models predict a positive response in every month. The monthly-mean temperature responses for individual models range from 1.5 K to 3 K during the winter and from 1.5 K to almost 5 K during the summer. It should be noted here that these coarse-resolution models may underestimate DJF temperature responses due to underestimating the magnitude of a snow-albedo feedback. This occurs because the extent of snow cover in the present climate is typically underestimated due to maximum elevations being unrealistically low.

Figs. 10a and 10b show the ratio of the all-model mean precipitation response to the standard deviation of the precipitation response over the 15 models, respectively in DJF and JJA over the continental U.S. This ratio is analogous to a signal to noise ratio, and measures the consistency of the response among the models. As one might expect after looking at Fig. 8, in JJA, the ratio is less than 1 everywhere in the U.S. This means that when all the models are considered, the predicted JJA precipitation response is

everywhere consistent with zero. In DJF, the all-model mean precipitation response is greater than the inter-model standard deviation only in some regions in the north of the continental U.S. / south of Canada and in one area of Mexico, where the amplitude of the response gets larger. This confirms that, over the U.S. at least, the predicted precipitation response to a doubling of CO_2 concentration is generally consistent with zero. The fact that the ratio is smaller in JJA than in DJF may reflect the fact that JJA precipitation typically is produced predominately by convection parameterization, whereas DJF precipitation is predominately large-scale. The different approaches to parameterizing convection in different models might lead to the tendency for the models to predict different JJA precipitation responses.

Another sort of signal to noise ratio can be defined as the ratio of simulated response to increased CO_2 divided by model error. In Figs 11a and 11b, we show, for DJF and JJA, respectively, this ratio for all-model mean near-surface temperature. In most regions of the U.S., the near-surface temperature response by this measure is highly significant. By contrast, for precipitation the same ratio is <1 in most locations, especially in DJF (Figs 11c and 11d).

Figs. 12 and 13 show the ratio of the all-model mean temperature response to the standard deviation of the temperature response over the 15 models, respectively in DJF and JJA over the U.S. As expected, both in DJF and JJA, the model-averaged temperature response is now greater than the inter-model standard deviation of that same response (ratio > 1) everywhere in the continental U.S. This shows that the models are consistent in predicting a positive temperature response everywhere in the U.S.

The results reported in this section are consistent with the general conclusions of the studies discussed in the introduction. Giorgi *et al.* (1994), Kim *et al.* (2002), Leung *et al.* (1999), and Snyder *et al.* (2002), who looked at the temperature and precipitation responses to increased CO_2 concentration over areas including partially or entirely the western U.S., found that over the western United States, the temperature response is significantly positive everywhere and in every month. They also generally found a small and negative precipitation response in summer and a larger positive response in winter, the statistical significance of the precipitation response being usually small. Kitter *et al.* (1998), who looked at the precipitation and temperature responses to doubled CO_2

concentration of nine models over seven subcontinental regions of the world, found that models agree on the positive temperature response but don't agree on the sign of the precipitation response over most regions.

3. Relationship between ability to simulate present climate and response to doubled CO_2 concentration

Different models simulate the present climate with different accuracies, and also predict different climate responses to a doubling of CO_2 concentration. The degree of agreement between a model's simulated present climate and observations is the main criterion on which models are evaluated. So one might wonder if models that simulate the present climate relatively well predict a different climate response to increased CO_2 concentration than models that are not as skillful. As discussed above, if this were true it would allow us to make refined estimates of the predicted climate responses to increased CO_2, and/or of the inter-model spread in those responses. In this section, we investigate possible relationships between the skill with which models simulate aspects of the present climate and their predicted response to a doubling of CO_2 concentration. We search for relationships between temperature or precipitation responses to increased CO_2 and spatio-temporal RMS model errors. The RMS errors are computed using:

$$RMS = \sqrt{\frac{\sum_N w_N \cdot (V_{\mathrm{mod},N} - V_{obs,N})^2}{\sum_N w_N}}$$

where:

- $V_{mod,N}$ is a simulated monthly mean temperature or precipitation over a specific grid cell of the area considered
- $V_{obs,N}$ is a monthly mean temperature or precipitation over a specific grid cell of the area considered, obtained respectively from reanalysis or observations
- N is the number of months (12) times the number of grid cells in the area considered (the summing is over all the grid cells and all the months)

- w_N is the area weight of a specific grid cell

For precipitation, three diagrams were plotted using the simulations of the 15 CMIP models. Fig. 14 represents the spatial and annual mean precipitation response versus the RMS error calculated over each grid cell and each month of the year, with respect to observations. Here the responses and RMS errors were calculated for latitudes 60 degrees S to 60 degrees N; we excluded the polar regions because these regions may have large errors but may not significantly influence the climate at lower latitudes. Fig. 15 represents the regional precipitation response over the western U.S., averaged over DJF, versus the same RMS error calculated over each grid cell between latitudes 60S and 60N, each month of the year. Fig. 16 represents the western U.S. precipitation response in DJF versus the RMS error calculated over a north-eastern Pacific region including the western U.S., each month of the year. This region is located between latitudes 0 degrees N and 60 degrees N, and longitudes 180 degrees W and 110 degrees W; it corresponds to the north-eastern Pacific where the weather patterns of the western U.S. are typically formed. These three diagrams do not show any obvious relationship between precipitation response and RMS error. The range of precipitation responses of the models with the smallest RMS errors also does not differ very much from the range of responses of the models with larger RMS errors.

To make this analysis more quantitative, we separated the models into two groups: the seven models with the smallest precipitation RMS errors in a specific region, and the seven models with the largest RMS errors in the same region. We compared model-mean responses, and the inter-model standard deviation of responses, between these two groups of models. Finally, we performed a 2-tailed t-test in each case between the precipitation responses of the models with the smallest RMS errors and the responses of the models with the largest RMS errors. The probability value obtained from the t-test on two sets of responses corresponds to the probability that the means of these two sets of values would be as different if they were randomly picked from the same distribution. Thus, a high probability value indicates that the mean response of the models with the smallest RMS errors cannot really be distinguished from the mean response of the models with the largest RMS errors. On the other hand, a low probability value (typically below 10 %)

indicates that the mean response of the models with small errors is significantly different from the mean response of the models with large errors. The model mean responses, standard deviations, probability values and t values are reported in Table 6.

	Mean response of 7 models with smallest RMS errors (mm/day)	Mean response of 7 models with largest RMS errors (mm/day)	Probability (%)	T value	Figure
Annual mean response over 60S to 60N, RMS error calculated over 60S to 60N	0.074 $\pm$ 0.033	0.050 $\pm$ 0.034	20	1.36	14
DJF response over western U.S., RMS error calculated over 60S to 60N	0.021 $\pm$ 0.465	0.480 $\pm$ 0.348	7	-1.98	15
DJF response over western U.S., RMS error calculated over North-Eastern Pacific region	0.221 $\pm$ 0.463	0.317 $\pm$ 0.472	71	-0.38	16

Table 6: Smallest RMS error model mean and largest RMS error model mean precipitation responses, and standard deviations of the responses over the different models. Probability values and t-values from the t-tests performed between the precipitation responses of the models with smallest RMS errors and the precipitation responses of the models with largest RMS errors

In each case, the inter-model variability (characterized by the standard deviation of the response over the different models) is comparable for the two groups of models. The probability value of 71 % in Table 6 confirms the absence of obvious relationship between the ability of the models to simulate the present climate precipitation over the north-eastern Pacific region and the precipitation response over the western U.S. in DJF. The low probability values given by the t-tests performed on the groups of responses of the models with low and high RMS error over the tropical and mid latitudes (60S to 60N) seem to indicate a relationship between the RMS error calculated over the region between latitudes 60 degrees S and 60 degrees N and the precipitation response over that same

region or over the western U.S. in DJF. Table 6, however, shows that the mean precipitation response for the two groups of models, both averaged over the region between latitudes 60S and 60N, are very close to each other (0.05 mm/day versus 0.074 mm/day while the inter-model variability is about 0.03 mm/day). And as far as the response over the western U.S. in DJF is concerned, the divergence between the models of small RMS error over the tropical to mid latitudes is such that no conclusion on the amplitude or even the sign of the precipitation response is possible. Therefore, for precipitation, we find that no matter whether we look at the regional response or the global response and no matter whether we consider the regional or the global simulation of present climate, it is not possible to narrow the range of predicted responses to doubled CO_2 concentration, by only considering the models that are best able to simulate precipitation in the present climate.

For temperature, a similar analysis (Figs. 17, 18, and 19) shows that neither the global annual mean temperature response nor the western U.S. regional response in DJF exhibit a relationship with the RMS error calculated over the region between latitudes 60 degrees S to 60 degrees N, over each month. However, the western U.S. response in DJF seems to show a relationship with the RMS error calculated over the north-eastern Pacific region (Fig. 19). This suggests that models with a superior ability to simulate surface temperatures in the region where weather systems of the western U.S. originate predict larger temperature responses to increased CO_2 in the western U.S. To see if a similar relationship holds for surface temperatures over Europe, we show a diagram of the DJF surface temperature response over Europe (latitudes between 35 degrees N and 60 degrees N, and longitudes between 10 degrees W and 30 degrees E) versus the RMS error calculated over the north-eastern Atlantic region (latitudes between 30 degrees N and 70 degrees N, and longitudes between 50 degrees W and 40 degrees E), over each month of the year. This shows a similar though noisier relation (Fig. 20). In both cases, the models with a smaller RMS error tend to predict a higher temperature response than the models with a larger RMS error in simulated surface temperatures. The significance of these relationships may be partially obscured by observational errors in ocean regions, which are typically larger than over land.

As with precipitation, temperature responses averaged over the seven models with the smallest RMS errors over the north-eastern Pacific region, the Northern Atlantic region, or the region between latitudes 60S and 60N and averaged over the seven models with the largest RMS errors, were calculated for the western U.S. or Europe in DJF, or annually for tropical to mid latitudes. The standard deviations of the temperature response over these two groups of seven models were calculated in each case as well. T-tests on the temperature responses were performed between the groups of models with the smallest RMS errors and the groups of models with the largest RMS errors. The results are reported in Table 7.

	Mean response of 7 models with smallest RMS errors (mm/day)	Mean response of 7 models with largest RMS errors (mm/day)	Probability (%)	T value	Figure
Annual mean response over 60S to 60N, RMS error calculated over 60S to 60N	1.574 $\pm$ 0.269	1.656 $\pm$ 0.251	87	–0.16	17
DJF response over western U.S., RMS error calculated over 60S to 60N	2.136 $\pm$ 0.228	2.156 $\pm$ 0.233	57	–0.58	18
DJF response over western U.S., RMS error calculated over North-Eastern Pacific region	2.346 $\pm$ 0.324	2.039 $\pm$ 0.237	7	2.02	19
DJF response over Europe, RMS error calculated over Northern Atlantic region	2.054 $\pm$ 0.270	1.861 $\pm$ 0.231	18	1.43	20

Table 7: Smallest RMS error model mean and largest RMS error model mean temperature responses, and standard deviations of the responses over the different models. Probability values and t-values from the t-tests performed between the temperature responses of the models with smallest RMS errors and the temperature responses of the models with largest RMS errors

Table 7 confirms the results obtained from Figs. 17 through 20: The models with the smallest RMS errors over the region between latitudes 60 degrees S and 60 degrees N have mean temperature responses over the western U.S. in DJF and over latitudes 60S to 60N and ranges of temperature responses very similar to the responses and ranges of responses of the models with the largest RMS errors. The high probability values (87 % and 57 %) obtained from the corresponding t-tests also show that in each case, the two groups of models predict similar mean responses. On the other hand, the t-test performed between the temperature responses of the models with the smallest RMS errors over the north-eastern Pacific region and the responses of the models with the largest RMS errors over that same region gives a small probability value (7 %). As suggested by Fig. 19, this shows that on average, the seven models with the smallest RMS error over the north-eastern Pacific region predict a significantly higher DJF temperature response over the western U.S. than the seven models with the biggest RMS error (2.35 K instead of 2.04 K). A probability value of 18 % for the t-test performed between the two sets of seven responses over Europe confirms that the models with the smallest RMS errors over the Northern Atlantic region also predict a significantly higher temperature response over Europe than the models with the largest RMS errors (2.05 K instead of 1.86 K). The higher probability value for Europe/Atlantic indicates that the relationship between RMS error and temperature response is not as strong as for the western U.S./Pacific (although, again, the significance of both of these relationships might be partly obscured by observational errors.)

Conclusion

The analysis of the present climate simulations in 15 global ocean-atmosphere-sea ice models shows some common features among the different models. The models tend to overestimate precipitation over the western U.S., especially in winter. Regarding the seasonal cycle of temperature, averaged over the western U.S., the models can be divided in three groups: those that overestimate the temperatures, especially in the summer, those that underestimate the temperatures in the winter / spring and generally overestimate the

temperatures in the summer, and finally those that agree well with reanalysis. The mean model generally manages to reproduce well the main spatial patterns of precipitation and temperature over the continental United States, and the misrepresentations are again often common to most models. For example, in DJF, the models tend to overestimate the winter precipitation in eastern Washington, eastern Oregon, Idaho, etc.; in JJA, they also displace westward the region of high precipitation in the Midwest. The overestimation of winter temperature in the north-eastern and north-central regions of the U.S. seems common to most models too; however, for temperature, there is a larger heterogeneity between the different models.

The analysis performed on the temperature and precipitation responses to a doubling of CO_2 concentration, over the western U.S. region, shows that there is no consensus between the different models for the amplitude and even the sign of the precipitation response. The temperature response, whose model-averaged amplitude ranges from 1.8 K to 2.8 K over the different months, presents a large inter-model variability. Nevertheless, this temperature response is consistently positive in the western U.S.

The 15 models studied have different abilities to simulate the present climate; they also have different temperature and precipitation responses to a doubling of CO_2 atmospheric concentrations. Although some relationships were found between the ability of the models to simulate accurately the present climate's precipitation (represented by the RMS errors) and the precipitation response to doubled CO_2 concentration, considering only the models that agree best with precipitation observations does not give a narrower range of precipitation responses. For temperature, some relationships seem to exist between the response over Europe or the western U.S. in DJF and the ability of the models to simulate the temperature respectively over the northern Atlantic or the north-eastern Pacific region. In both cases, the more accurate models predict a larger temperature response.

This result has important implications. It means that it is difficult to narrow the range of predicted responses to increased CO_2 concentration by just considering the models that have the best ability to simulate the present climate. Also, climate models are typically evaluated based on how well they reproduce the present climate; however, for precipitation, and to some extent for temperature as well, "better" models do not give a

different prediction of the response to increased CO_2 concentration than "worse" models. This would seem to undercut the common assumption that models that are better at simulating the present climate will give better predictions of future climate. This conclusion, however, only applies among models of already high quality. It is obvious that beyond a certain level, models of poor quality will not be able to predict a response in the best models' range of responses other than by chance. Also, we only compared the model results to one set of observational data for precipitation and to two sets of reanalysis data for temperature. A study based on other sets of reference data might come to different conclusions as observations and reanalysis data sometimes largely differ from one another. And finally, our study was limited to temperature and precipitation over a few regions and we cannot generalize our conclusions to other variables or other regions of the world.

Acknowledgements:

This work was performed under the auspices of the U.S. Department of Energy by the Lawrence Livermore National Laboratory under contract No. W-7405-Eng-48. We thank Drs. C. Covey and B.D. Santer for their interest in this work and helpful suggestions. We also thank C. Doutriaux for his technical contributions to several aspects of the analysis.

Tables

Model	**Institution/Country**	**Control Run CO2 [ppmv]**	**Atmospheric Resolution**	**Ocean Resolution**
GFDL_R15_a	GFDL/USA	360	R15 (4.5 x 7.5) L9	4.5 x 3.7 L12
GOALS	LASG/China	345	R15 (4.5 x 7.5) L9	4.0 x 5.0 L20

ECHAM3/LSG	ECMWF/UK	345	T21 (5.6 x 5.6) L19	4.0 x 4.0 L11
CCSR/NIES	Univ. of Tokyo/Japan	345	T21 (5.6 x 5.6) L20	2.8 x 2.8 L17
GISS2	NASA-GISSS/USA	315	4.0 x 5.0 L9	4.0 x 5.0 L13
MRI1	Meteorological Res. Inst./Japan	345	4.0 x 5.0 L15	2.0 x 2.5 L21
IPSL-CM2	IPSL/France	320	5.6 x 3.8 L15	2.0 x 2.0 L31
BMRCb	BMRC/Australia	330	R21 (3.2 x 5.6) L17	3.2 x 5.6 L12
CSIRO Mk2	CSIRO/Australia	330	R21 (3.2 x 5.6) L9	3.2 x 5.6 L21
ARPEGE/OPA2	CERFACS/France	353	T31 (3.9 x 3.9) L19	2.0 x 2.0 L31
CGCM1	CCCMA/Canada	330	T32 (3.8 x 3.8) L10	1.8 x 1.8 L29
HadCM3	UKMO/UK	289.6	2.5 x 3.75 L19	1.25 x 1.25 L20
HadCM2	UKMO/UK	322.6	2.5 x 3.75 L19	2.5 x 3.75 L20
CSM1.0	NCAR/USA	355	T42 (2.8 x 2.8) L18	2.0 x 2.4 L45
DOE PCM	NCAR	355	T42 (2.8 x 2.8) L18	0.67 x 0.67 L32

Table 1: List of the 15 CMIP models with their control run CO_2 concentration, atmospheric resolution and ocean resolution. Models are listed in order of number of horizontal grid cells in the atmospheric component.

DJF

rank	model	RMS error
1	HadCM3	0.93
2	DOE PCM	0.94
3	CSM 1.0	0.97
4	HadCM2	1.03
5	CCSR/NIES	1.12
6	GISS2	1.15
7	CSIR0 Mk2	1.15
8	ECHAM3/LSG	1.22
9	ARPEGE/OPA2	1.28
10	MRI1	1.29
11	GOALS	1.37
12	CGCM1	1.40
13	GFDL_R15_a	1.44
14	IPSL-CM2	1.66
15	BMRCb	1.70

JJA

rank	model	RMS error
1	HadCM3	0.75
2	HadCM2	O.93
3	CSIRO Mk2	1.02
4	ARPEGE/OPA2	1.06
5	GOALS	1.12
6	ECHAM3/LSG	1.19
7	CSM 1.0	1.29
8	GFDL_R15_a	1.37
9	BMRCb	1.38
10	GISS2	1.50
11	DOE PCM	1.55
12	CCSR/NIES	1.57
13	IPSL-CM2	1.75
14	MRI1	1.76
15	CGCM1	1.88

Tables 2 and 3: RMS errors of the precipitation over the U.S. in DJF and JJA respectively, calculated for each model with respect to observations.

DJF

rank	model	RMS error
1	DOE PCM	1.79
2	CSM 1.0	1.85
3	HadCM3	1.90
4	CSIRO Mk2	1.92
5	GFDL_R15_a	2.15
6	ECHAM3/LSG	2.24
7	BMRCb	2.43
8	CCSR/NIES	2.62
9	HadCM2	2.96
10	CGCM1	3.07
11	MRI1	3.28
12	GISS2	3.31
13	ARPEGE/OPA2	3.38
14	GOALS	3.58
15	IPSL-CM2	3.81

JJA

rank	model	RMS error
1	HadCM3	1.34
2	CGCM1	1.58
3	CSIRO Mk2	1.61
4	HadCM2	1.85
5	CSM 1.0	1.87
6	DOE PCM	1.95
7	ARPEGE/OPA2	2.32
8	GISS2	2.40
9	GFDL_R15_a	2.53
10	ECHAM3/LSG	2.64
11	IPSL-CM2	2.80
12	CCSR/NIES	3.47
13	BMRCb	3.81
14	GOALS	4.63
15	MRI1	5.22

Tables 4 and 5: RMS errors of the temperature over the U.S. in DJF and JJA respectively, calculated for each model with respect to reanalysis.

	Mean response of 7 models with smallest RMS errors (mm/day)	Mean response of 7 models with largest RMS errors (mm/day)	Probability (%)	T value	Figure
Annual mean response over 60S to 60N, RMS error calculated over 60S to 60N	0.074 ± 0.033	0.050 ± 0.034	20	1.36	14
DJF response over western U.S., RMS error calculated over 60S to 60N	0.021 ± 0.465	0.480 ± 0.348	7	-1.98	15
DJF response over western U.S., RMS error calculated over North-Eastern Pacific region	0.221 ± 0.463	0.317 ± 0.472	71	-0.38	16

Table 6: Smallest RMS error model mean and largest RMS error model mean precipitation responses, and standard deviations of the responses over the different models. Probability values and t-values from the t-tests performed between the precipitation responses of the models with smallest RMS errors and the precipitation responses of the models with largest RMS errors.

	Mean response of 7 models with smallest RMS errors (mm/day)	Mean response of 7 models with largest RMS errors (mm/day)	Probability (%)	T value	Figure
Annual mean response over 60S to 60N, RMS error calculated over 60S to 60N	1.574 ± 0.269	1.656 ± 0.251	87	-0.16	17
DJF response over western U.S., RMS error calculated over 60S to 60N	2.136 ± 0.228	2.156 ± 0.233	57	-0.58	18
DJF response over western U.S., RMS error calculated over North-Eastern Pacific region	2.346 ± 0.324	2.039 ± 0.237	7	2.02	19

DJF response over Europe, RMS error calculated over Northern Atlantic region	2.054 ± 0.270	1.861 ± 0.231	18	1.43	20

Table 7: Smallest RMS error model mean and largest RMS error model mean temperature responses, and standard deviations of the responses over the different models. Probability values and t-values from the t-tests performed between the temperature responses of the models with smallest RMS errors and the temperature responses of the models with largest RMS errors

Figure Captions

Fig 1: Seasonal cycles of present climate precipitation over the western U.S., predicted by the 15 CMIP models (red) and compared to the CMAP observations [2] (green). The error bars extend one standard deviation (calculated over the individual years considered) on either side of the monthly means.

Fig. 2: Seasonal cycle of all-model mean present climate precipitation over the western U.S. (in red), compared to the CMAP observations [2] (in green). The error bars extend one standard deviation (calculated over the 15 models) on either side of the monthly means.

Figure 3a: Comparison of near-surface temperatures in the Western U.S., in several reanalysis data sets (NCEP, NCEP2, NASA, ECMWF) and two observational data sets (UW and VEMAP).

Fig. 3b: Seasonal cycles of present climate temperature over the western U.S., predicted by the 15 CMIP models (red) and compared to the NCEP2 reanalysis [3] (yellow). The error bars extend one standard deviation (calculated over the individual years considered) on either side of the monthly means.

Fig. 4a: Present climate precipitation observations over the United States in DJF

Fig. 4b: All model mean present climate precipitation over the United States in DJF

Fig. 4c: All model mean present climate DJF precipitation minus observed DJF precipitation

Fig. 4d: For DJF precipitation, all-model mean minus observed precipitation, divided by observed interannual variability.

Fig. 5a: Same as Figure 4a, for JJA

Fig. 5b: Same as Figure 4b, for JJA

Fig. 5c: Same as Figure 4c, for JJA

Fig 5d: Same as Figure 4d, for JJA

Fig. 6a: Present climate temperature over the United States in DJF, given by the NCEP2 reanalysis

Fig. 6b: All model mean present climate temperature over the United States in DJF

Fig. 6c: All model mean present climate DJF temperature minus NCEP2 reanalysis DJF temperature

Fig. 6d: Root mean square difference between model and NCEP2 reanalysis DJF present climate temperature, calculated over the 15 CMIP models

Fig. 6e: For DJF near-surface temperature: all model mean minus NCEP2 reanalysis, divided by observed interannual variability.

Fig. 7a: Same as Figure 6a, for JJA

Fig. 7b: Same as Figure 6b, for JJA

Fig. 7c: Same as Fig. 6c, for JJA

Fig. 7d: Same as Fig. 6d, for JJA

Fig. 7e: Same as Fig. 6e, for JJA

Figs. 8a and 8b: Seasonal cycle of the precipitation response to doubled CO_2 concentration over the western U.S., averaged over the 15 CMIP models, and standard deviation of the response over the different models. Top: response in mm/day. Bottom: response as a fraction of monthly present-day precipitation

Fig 9: Same as Fig. 8a for the near-surface temperature response

Fig 10a: Ratio of the all-model mean DJF precipitation response (to doubled CO_2 atmospheric concentration) to the standard deviation of the response over the 15 models

Fig 10b: Same as Fig 10, for the JJA precipitation response.

Fig. 11a: All-model mean response in near-surface temperature to increased CO_2, divided by error in all-model mean near-surface temperature, for DJF.

Fig. 11b: Same as Fig. 11a, for JJA.

Fig. 11c: All-model mean response in precipitation to increased CO_2, divided by error in all-model mean precipitation, for DJF.

Fig. 11d: Same as Fig. 11c, for JJA.

Fig 12: Same as Fig 10, for the DJF near-surface temperature response

Fig 13: Same as Fig 10, for the JJA near-surface temperature response.

Fig. 14: Annual mean precipitation response to doubled CO_2 atmospheric concentration, over latitudes 60S to 60N versus RMS error calculated over the same region, over each month of the year

Fig. 15: Precipitation response to doubled CO_2 atmospheric concentration, over the western U.S. in DJF versus RMS error calculated over latitudes 60S to 60N, over each month of the year

Fig. 16: Precipitation response to doubled CO_2 atmospheric concentration, over the western U.S. in DJF versus RMS error calculated over the North-Eastern Pacific region, over each month of the year

Fig. 17: Response of annual mean near-surface temperature to doubled CO_2 atmospheric concentration, over latitudes 60S to 60N versus RMS error calculated over the same region, over each month of the year

Fig. 18: Response of near-surface temperature to doubled CO_2 atmospheric concentration, over the western U.S. in DJF versus RMS error calculated over latitudes 60S to 60N, over each month of the year

Fig. 19: Temperature response to doubled CO_2 atmospheric concentration, over the western U.S. in DJF versus RMS error calculated over the North-Eastern Pacific region, over each month of the year.

Fig. 20: Temperature response to doubled CO_2 atmospheric concentration, over Europe in DJF versus RMS error calculated over the Northern Atlantic region, over each month of the year

References:

Climate Prediction Center Merged Analysis of Precipitation (CMAP), http://www.cpc.ncep.noaa.gov/products/global_precip/html/wpage.cmap.html

Coupled Model Intercomparison Project (CMIP), http://www-DOE PCMdi.llnl.gov/cmip/

Covey C, AchutaRao KM, Cubasch U, Jones P, Lambert SJ, Mann ME, Phillips TJ, and Taylor KE, (2003) An overview of results from the Coupled Model Intercomparison Project. Global and Planetary Change 37: 103-133

Duffy P B, Govindasamy B, Iorio J, Milovich J, Taylor K, Wehner M, and Thompson S, (2003) High Resolution Simulations of Global Climate, Part 1: Present Climate. Climate Dynamics 21:371-390.

European Center for Medium-Range Weather Forecast ERA15 Reanalysis, http://www.ecmwf.int/research/era/ERA-15/

Giorgi F, Brodeur SC, and Bates GT (1994) Regional climate change scenarios over the United States produced with a nested Regional Climate Model. Journal of Climate 7: 375-399.

Kim J, Kim TK, Arritt RW, Miller NL (2002) Impacts of increased atmospheric CO_2 on the hydroclimate of the western United States. Journal of Climate 15 1926-1942.

Kittel TGF, Giorgi F, Meehl GA (1998) Intercomparison of regional biaises and doubled CO_2-sensitivity of coupled atmosphere-ocean general circulation model experiments. Climate Dynamics 14: 1-15.

Leung LR, and Ghan SJ (1999) Pacific Northwest climate sensitivity simulated by a Regional Climate Model driven by a GCM. Part II: $2xCO_2$ simulations. Journal of Climate 12: 2031-2053.

NCEP /DOE AMIP-II Reanalysis, http://wesley.wwb.noaa.gov/reanalysis2/index.html

Snyder MA, Bell, JL, Sloan LC, Duffy PB, and Govindasamy B (2002) Climate responses to a doubling of atmospheric carbon dioxide for a climatically vulnerable region. Geophysical Research Letters 29: 1-4.

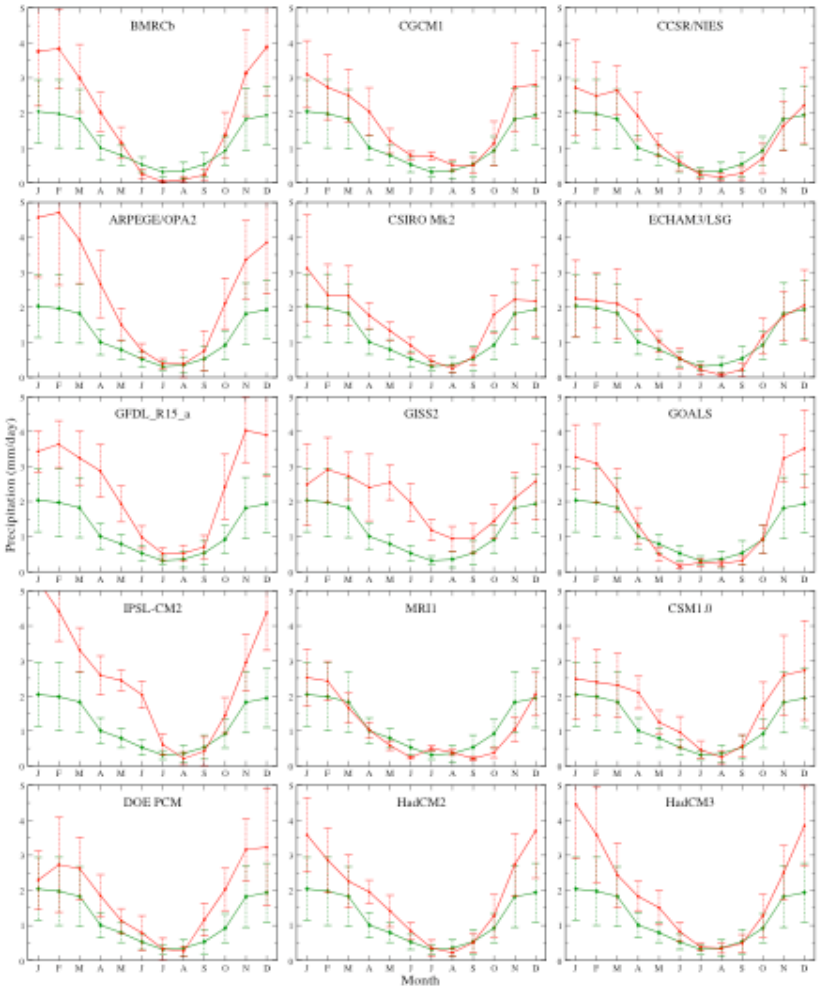

Fig 1: Seasonal cycles of present climate precipitation over the western U.S., predicted by the 15 CMIP models (red) and compared to the CMAP observations [2] (green). The error bars extend one standard deviation (calculated over the individual years considered) on either side of the monthly means.

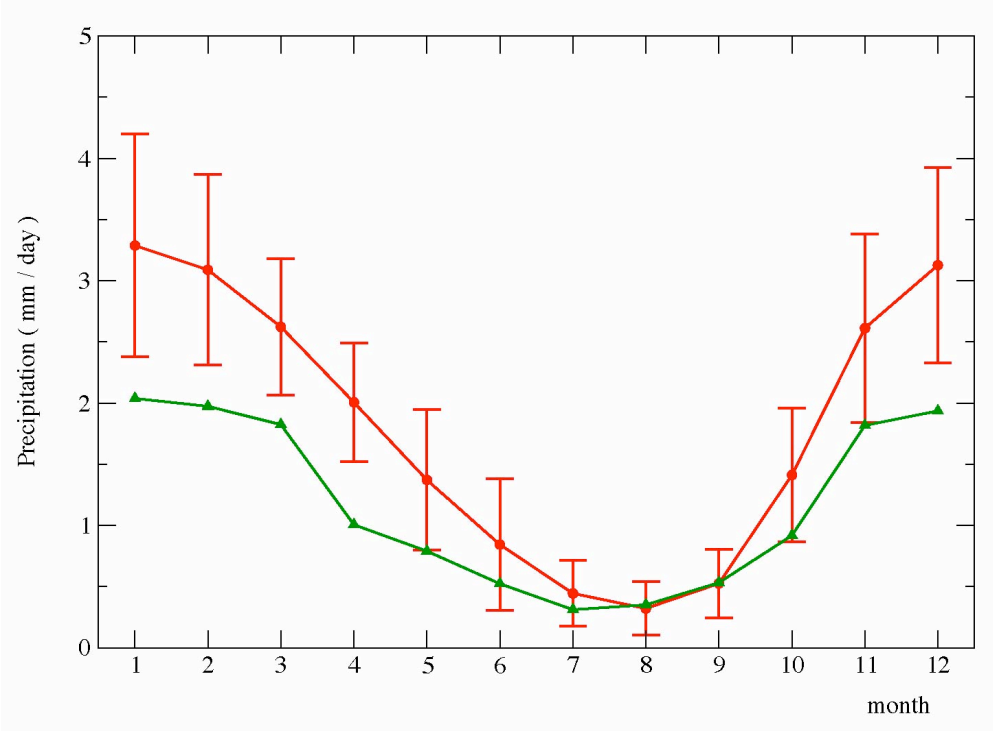

Fig. 2: Seasonal cycle of all-model mean present climate precipitation over the western U.S. (in red), compared to the CMAP observations [2] (in green). The error bars extend one standard deviation (calculated over the 15 models) on either side of the monthly means.

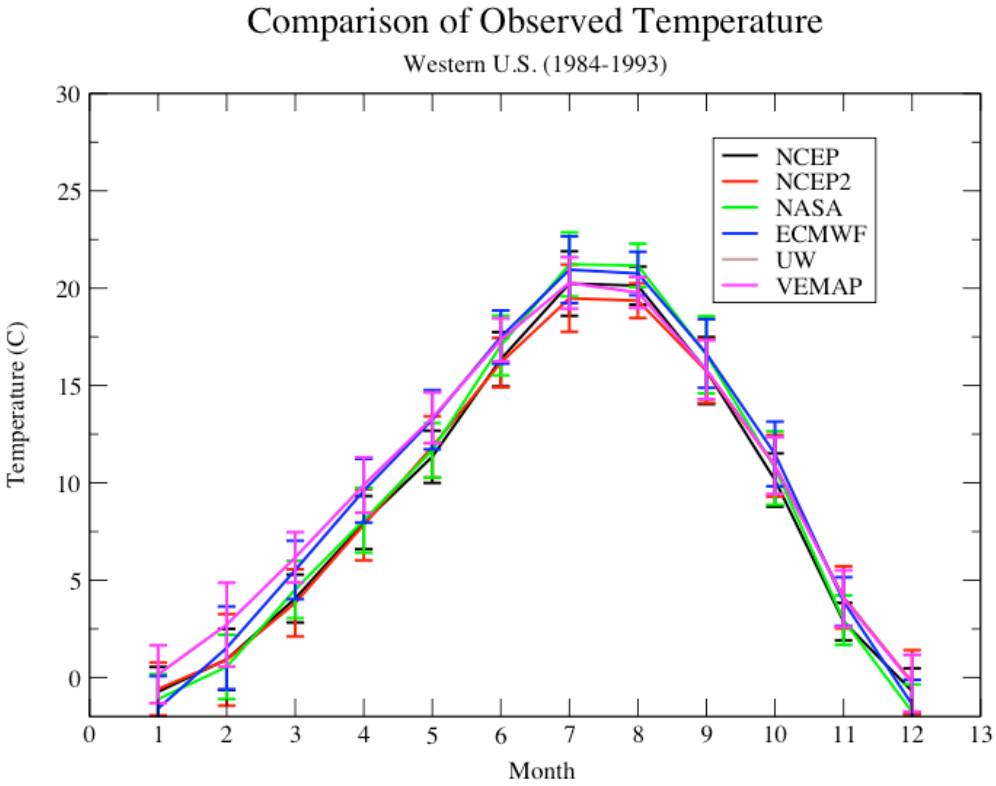

Figure 3a: Comparison of near-surface temperatures in the Western U.S., in several reanalysis data sets (NCEP, NCEP2, NASA, ECMWF) and two observational data sets (UW and VEMAP).

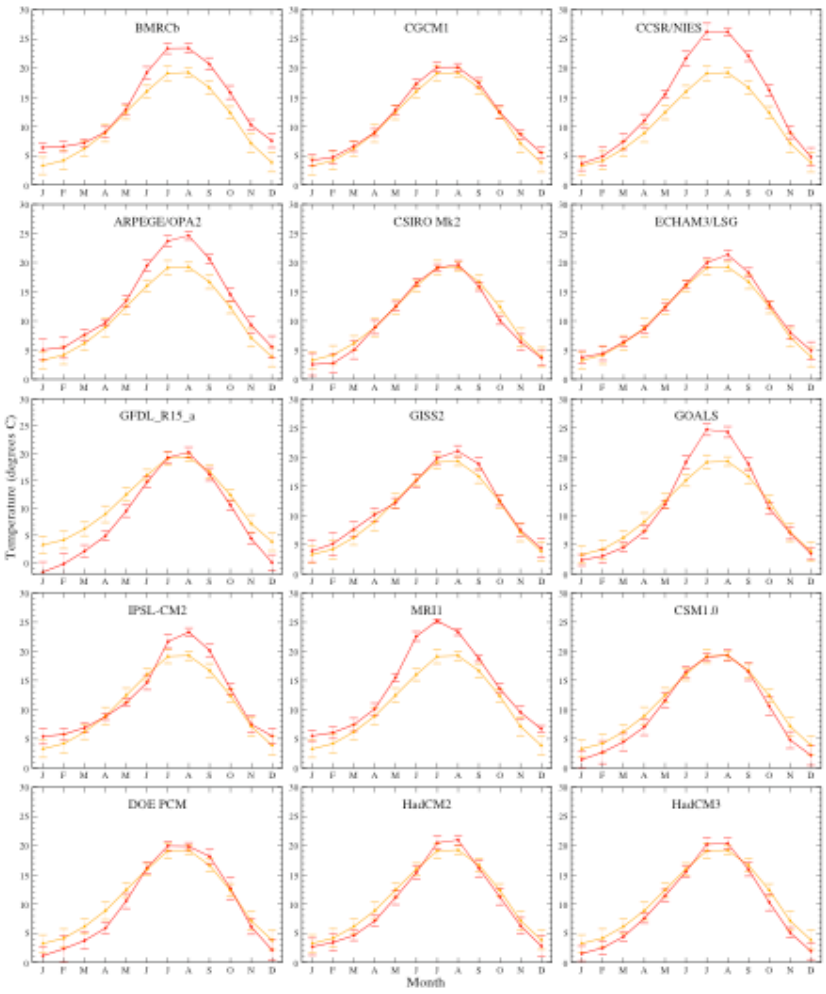

Fig. 3b: Seasonal cycles of present climate temperature over the western U.S., predicted by the 15 CMIP models (red) and compared to the NCEP2 reanalysis [3] (yellow). The error bars extend one standard deviation (calculated over the individual years considered) on either side of the monthly means.

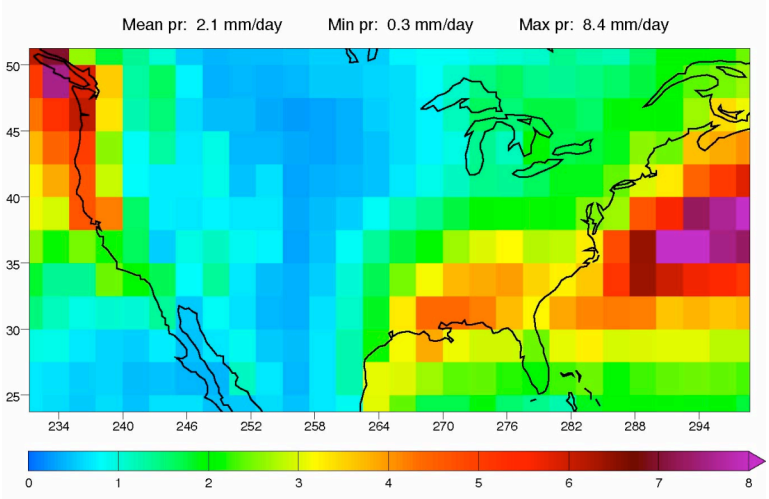

Fig. 4a: Present climate precipitation observations over the United States in DJF

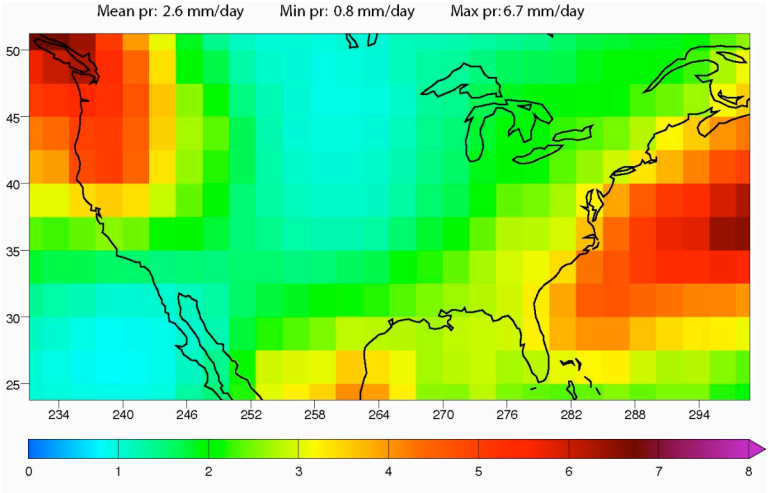

Fig. 4b: All model mean present climate precipitation over the United States in DJF

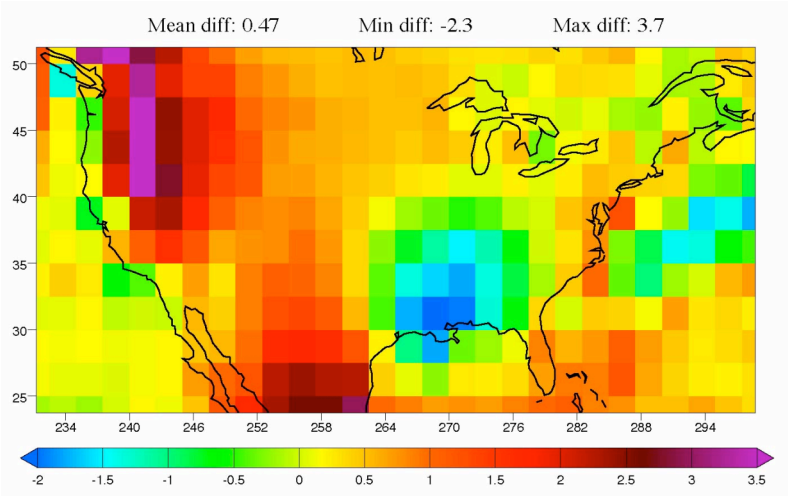

Fig. 4c: All model mean present climate DJF precipitation minus observed DJF precipitation

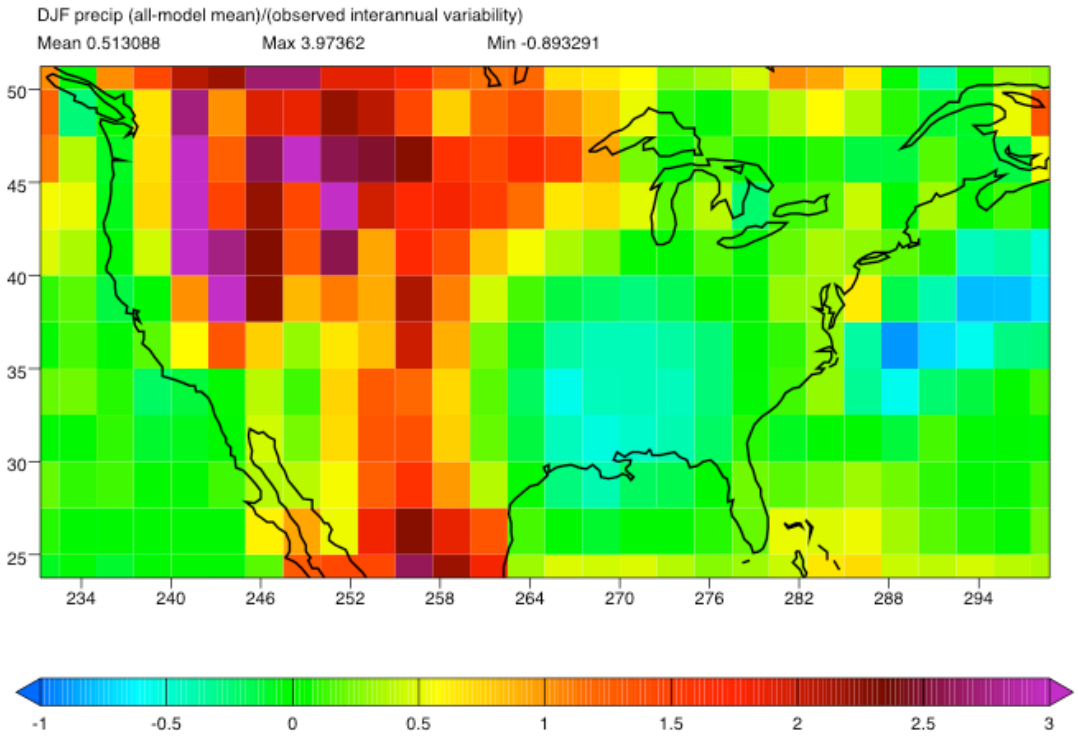

Fig. 4d: For DJF precipitation, all-model mean minus observed precipitation, divided by observed interannual variability.

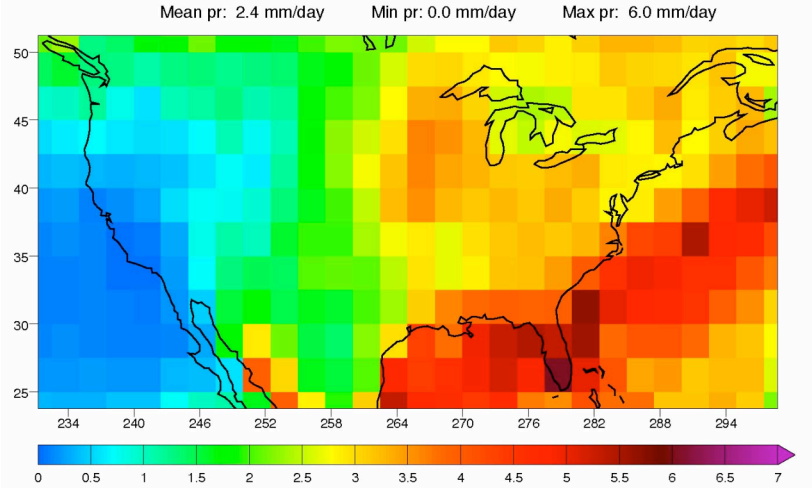

Fig. 5a: Same as Figure 4a, for JJA

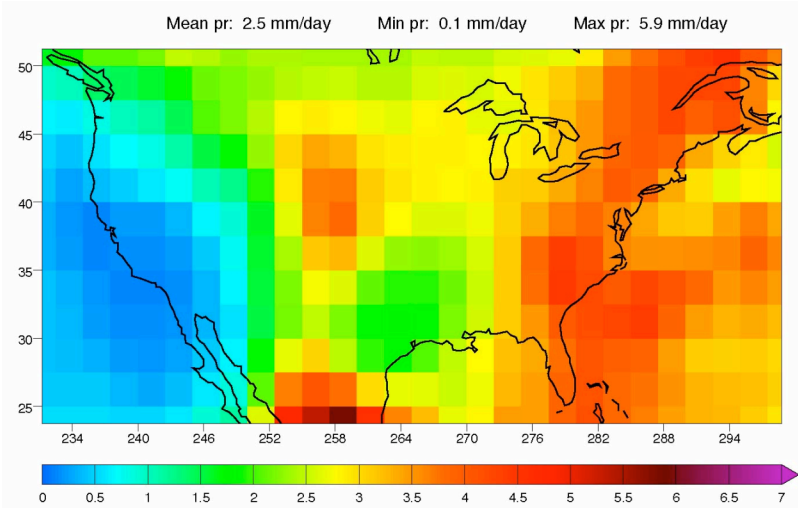

Fig. 5b: Same as Figure 4b, for JJA

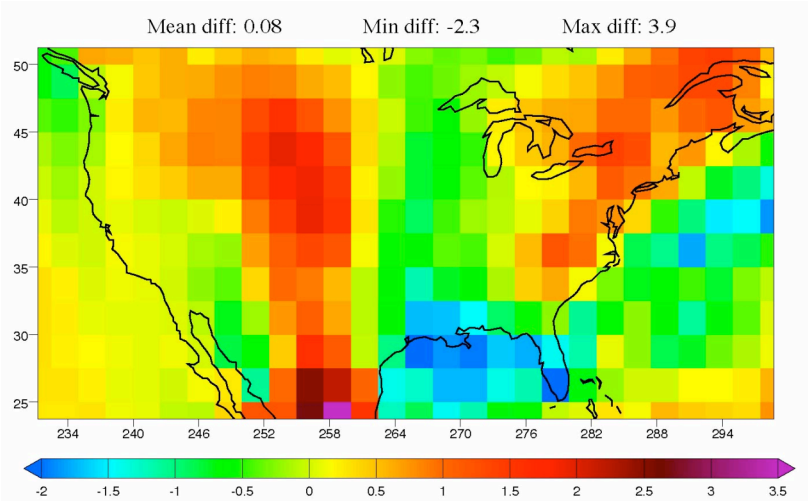

Fig. 5c: Same as Figure 4c, for JJA

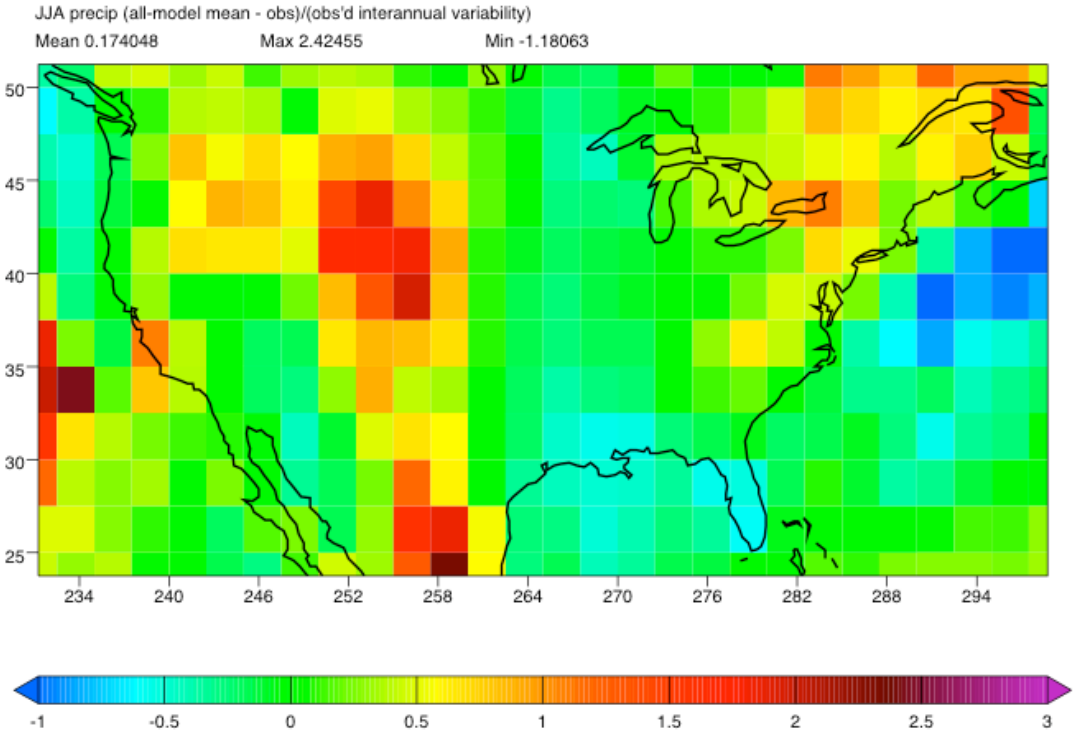

Fig. 5d: Same as Figure 4d, for JJA

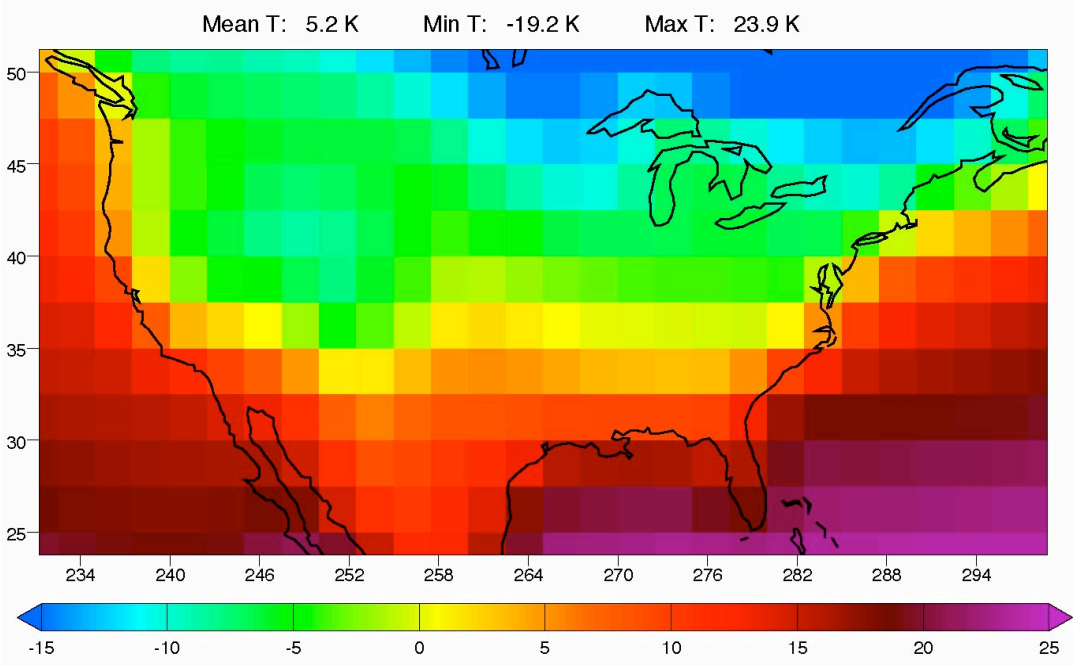

Fig. 6a: Present climate temperature over the United States in DJF, given by the NCEP2 reanalysis

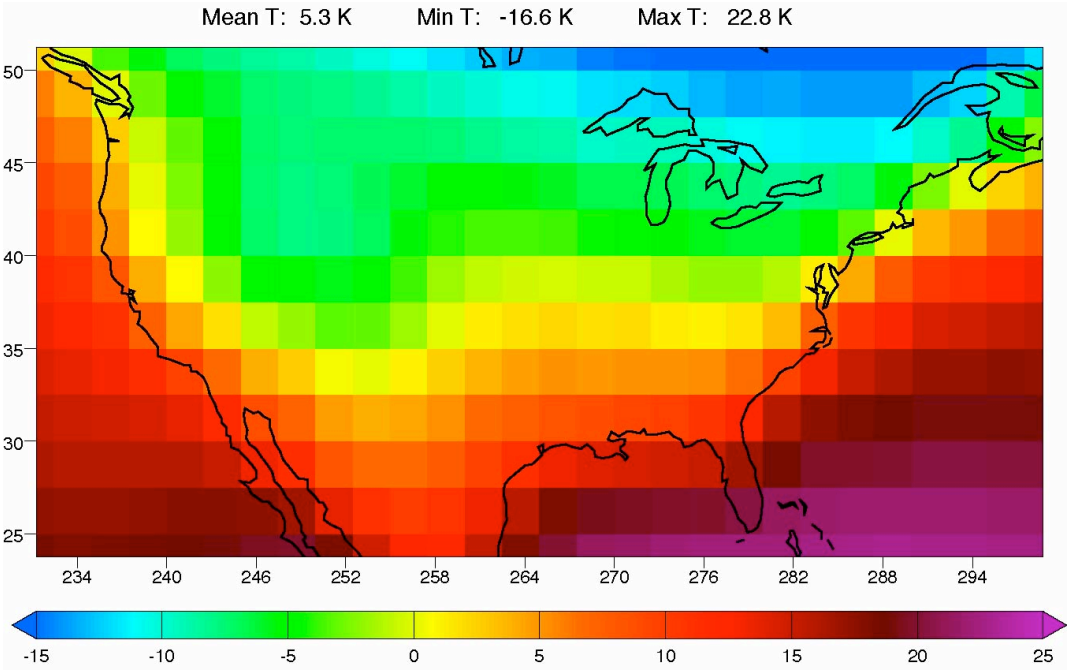

Fig. 6b: All model mean present climate near-surface temperature over the United States in DJF

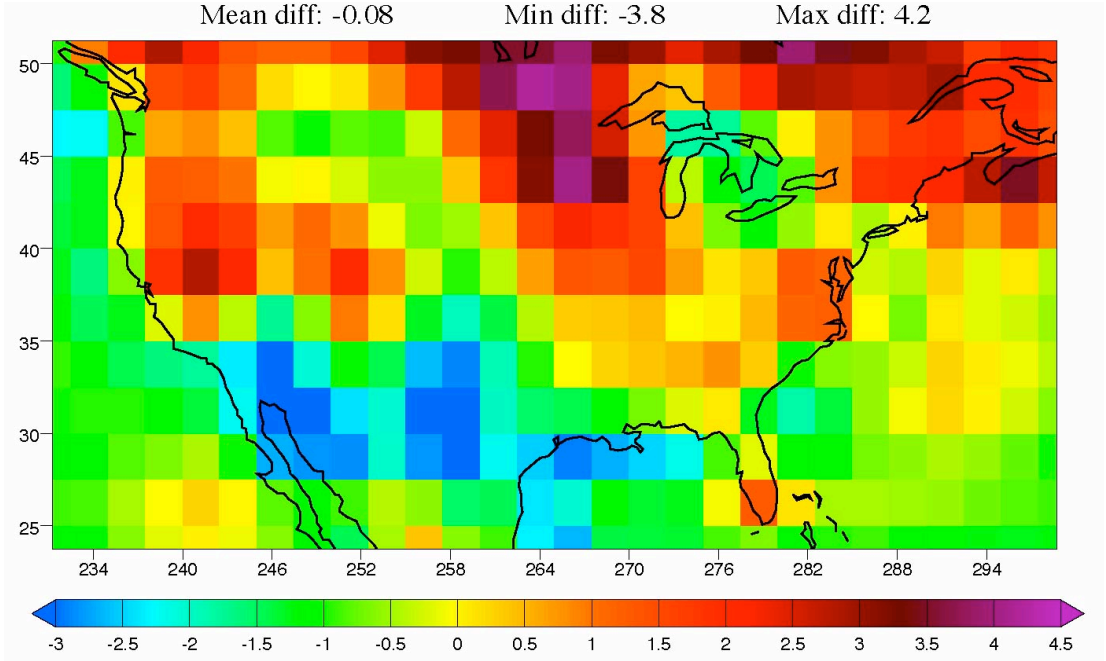

Fig. 6c: All model mean present climate DJF temperature minus NCEP2 reanalysis DJF temperature

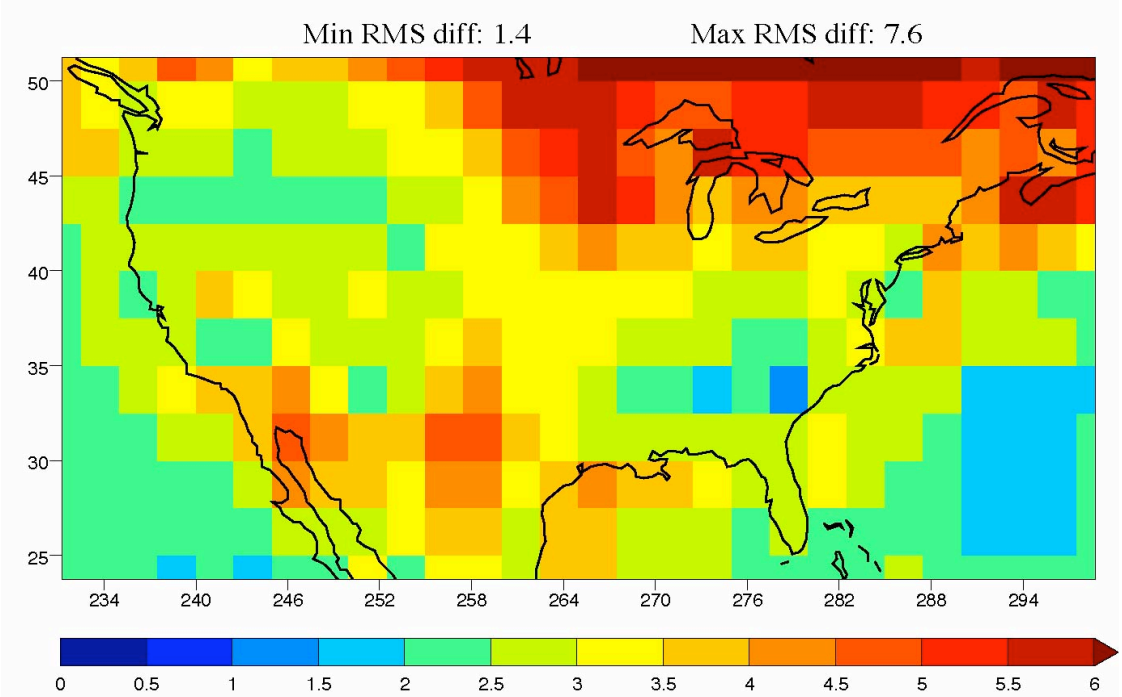

Fig. 6d: Root mean square difference between model and NCEP2 reanalysis DJF present climate temperature, calculated over the 15 CMIP models

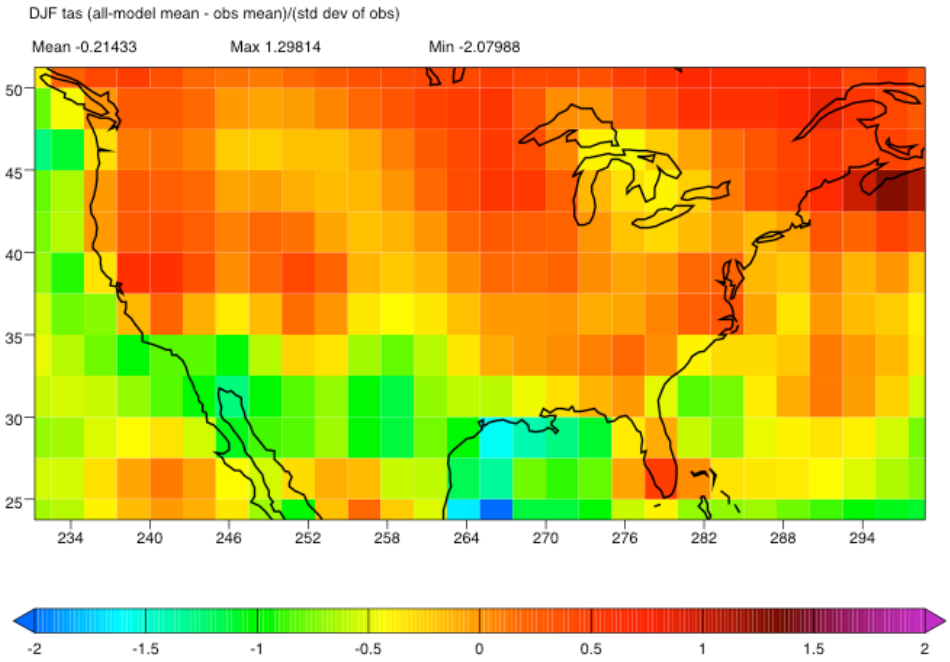

Fig. 6e: For DJF near-surface temperature: all model mean minus NCEP2 reanalysis, divided by observed interannual variability.

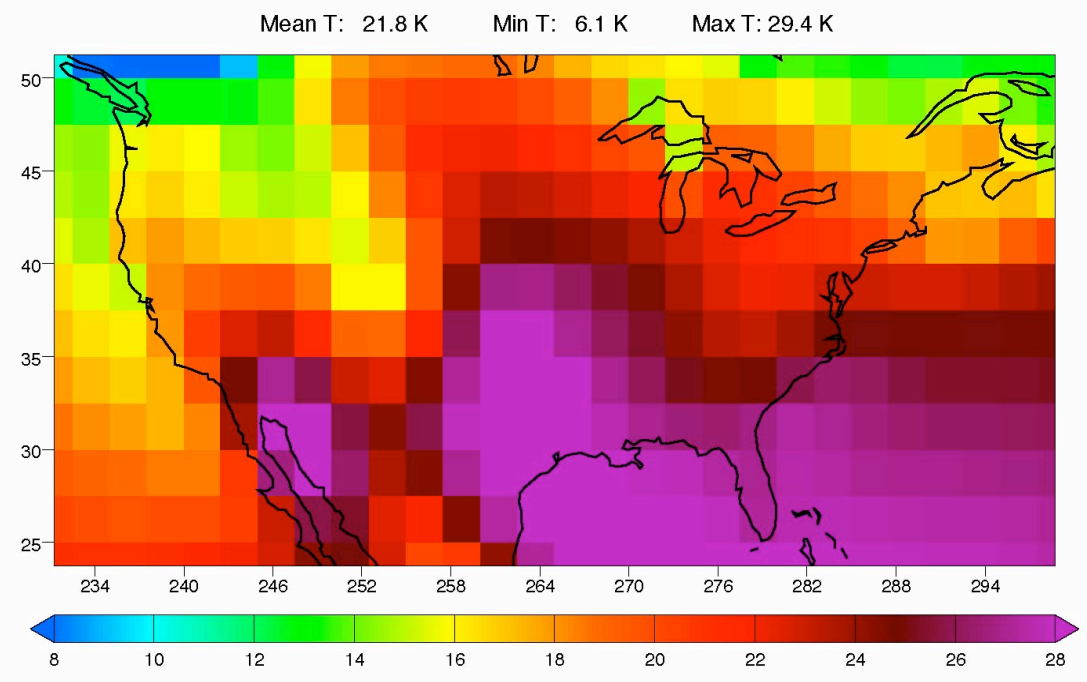

Fig. 7a: Same as Figure 6a, for JJA

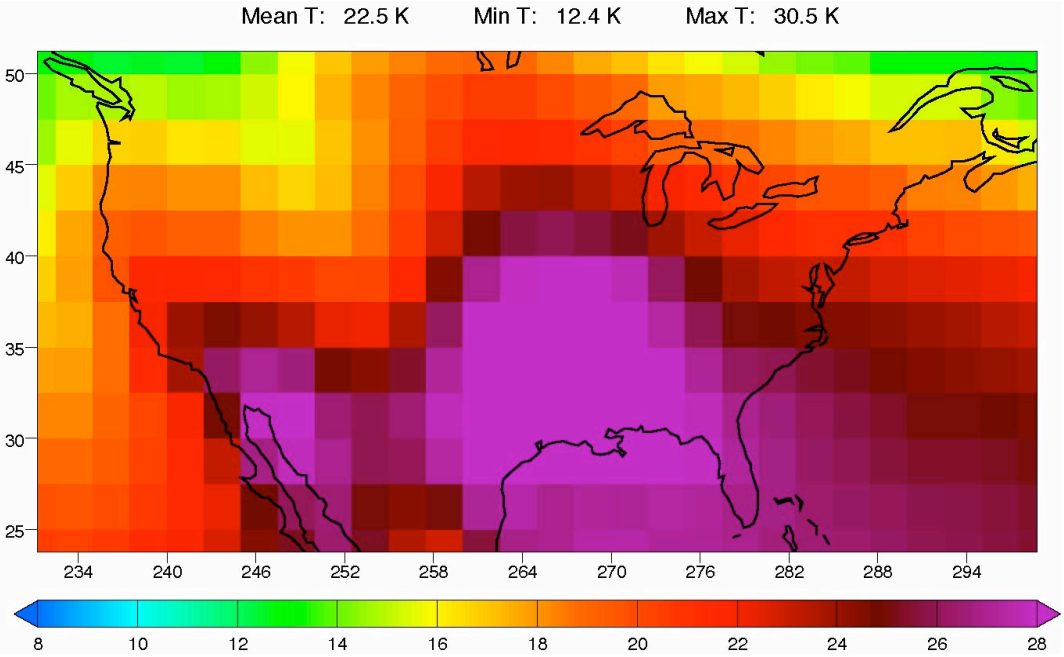

Fig. 7b: Same as Figure 6b, for JJA

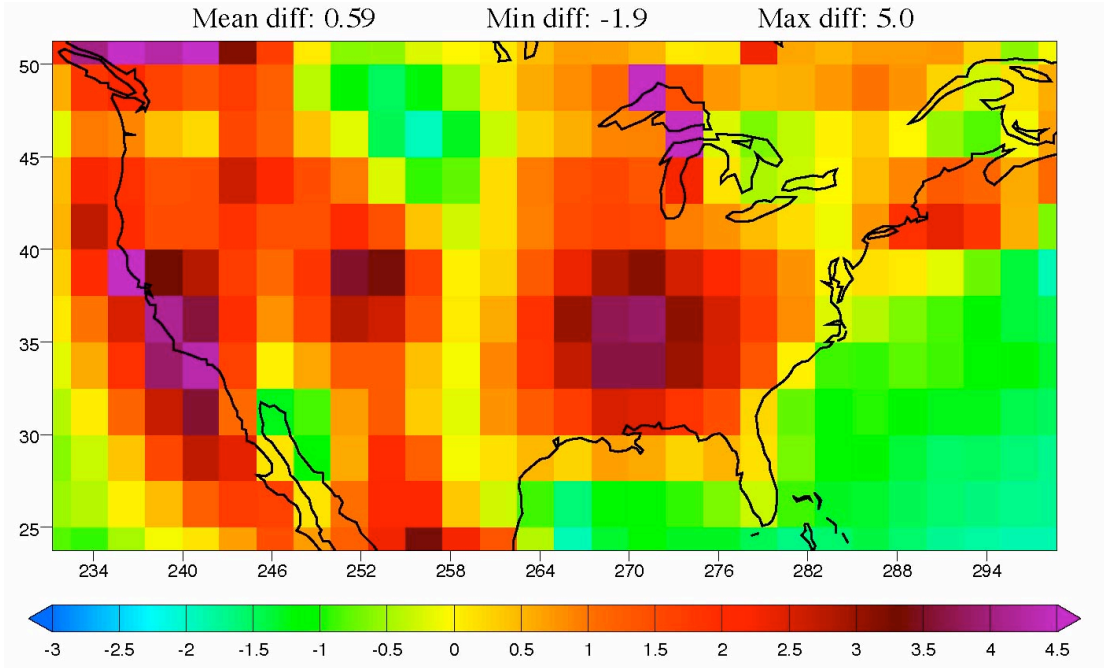

Fig. 7c: Same as Fig. 6c, for JJA

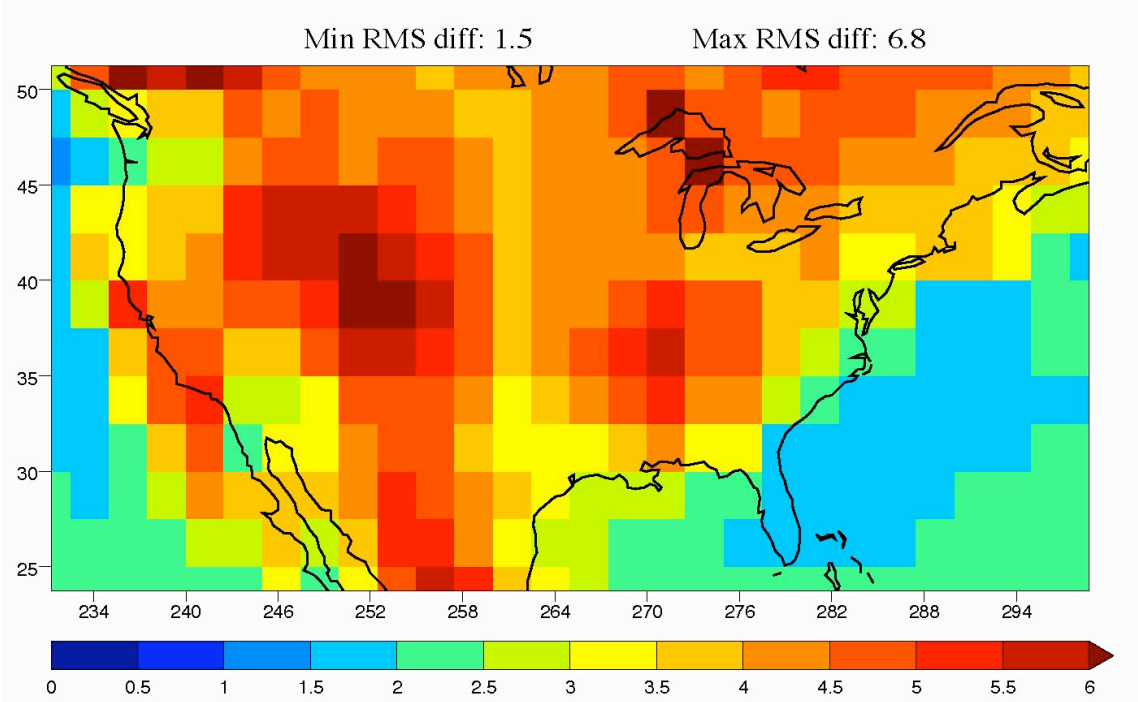

Fig. 7d: Same as Fig. 6d, for JJA

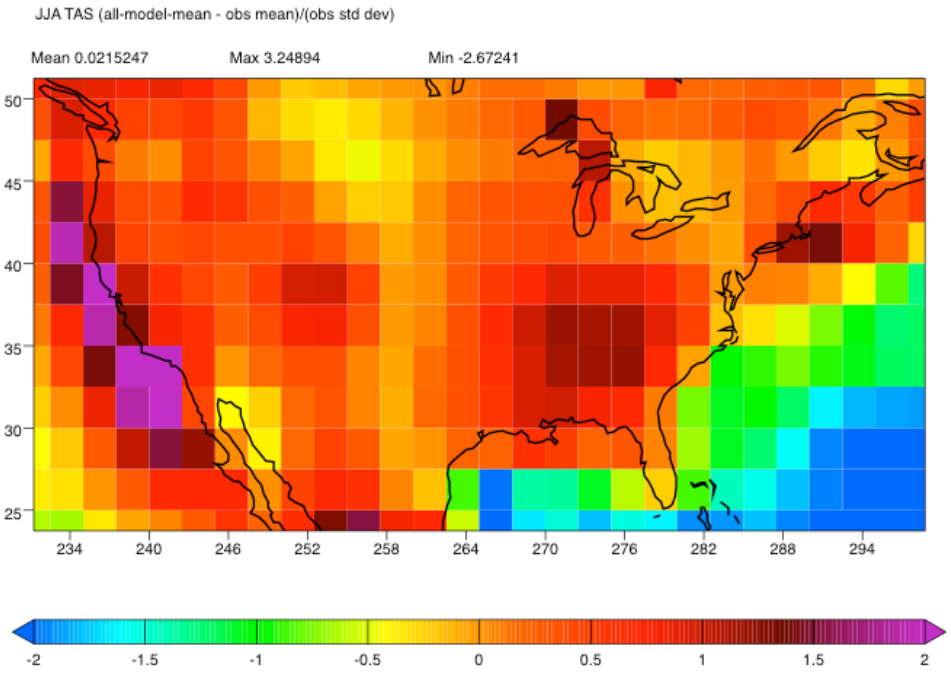

Fig. 7e: Same as Fig. 6e, for JJA

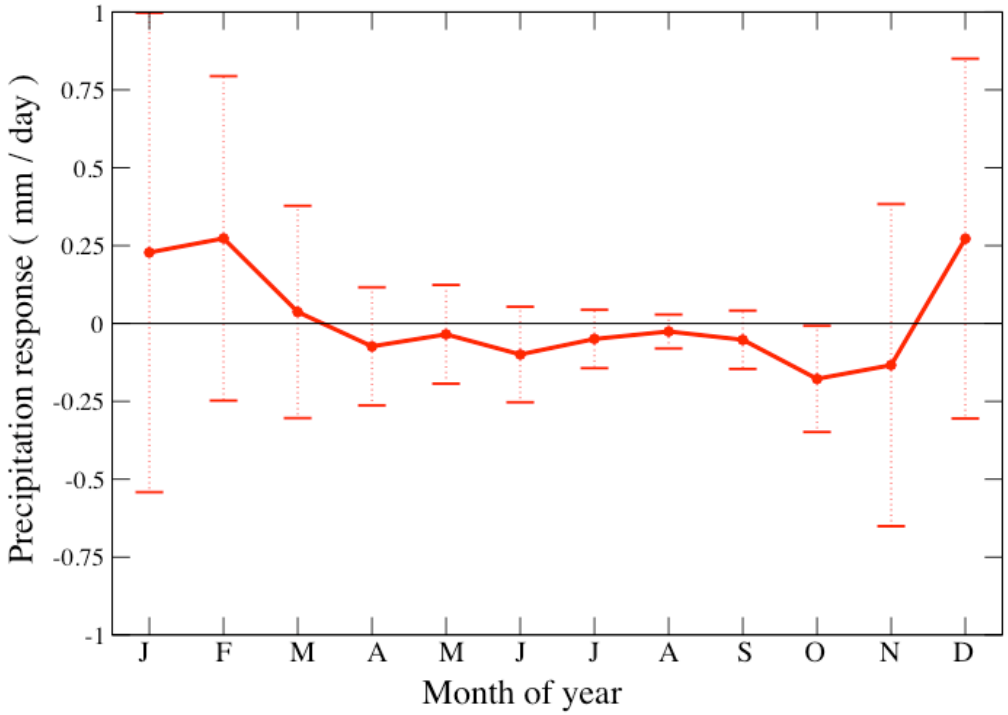

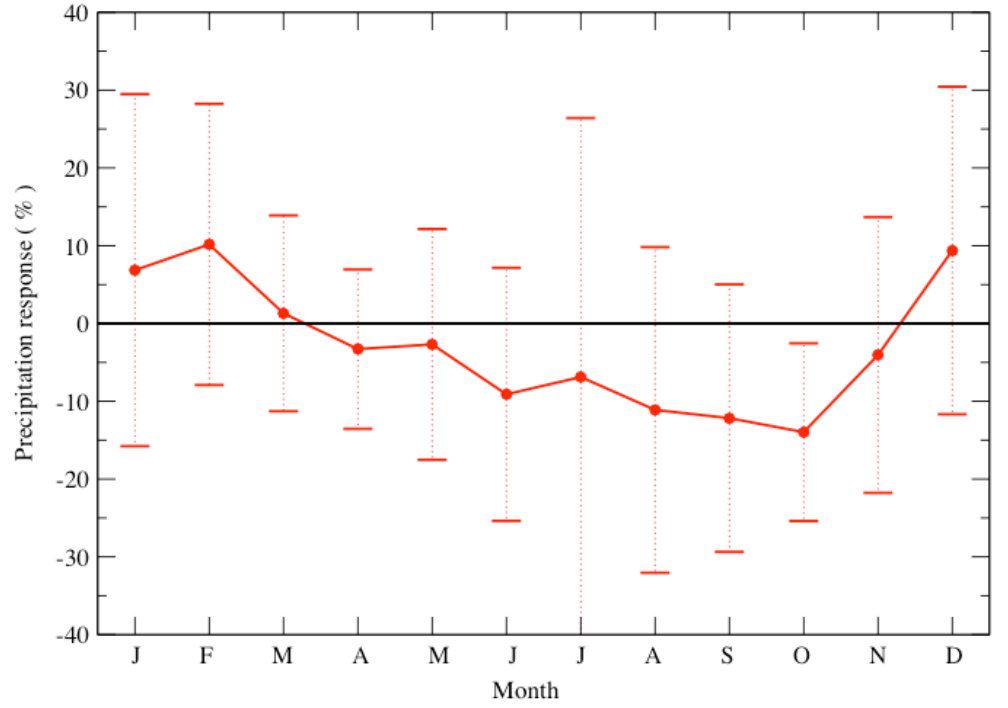

Figs. 8a and 8b: Seasonal cycle of the precipitation response to doubled CO_2 concentration over the western U.S., averaged over the 15 CMIP models, and standard deviation of the response over the different models. Top: response in mm/day. Bottom: response as a fraction of monthly present-day precipitation

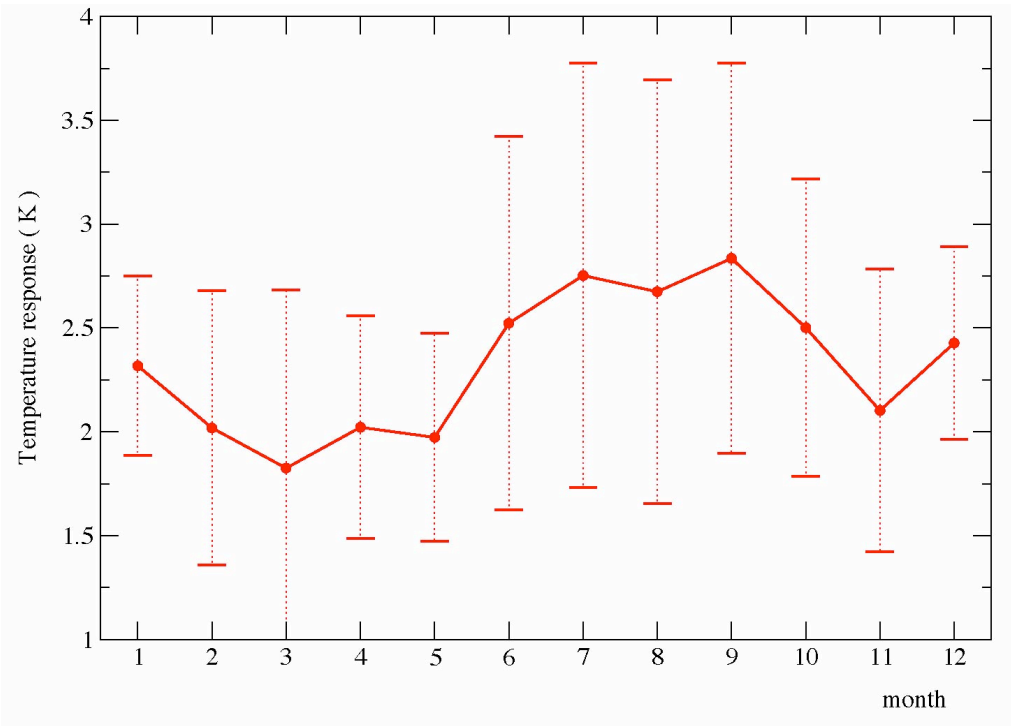

Fig 9: Same as Fig. 8a for the temperature response

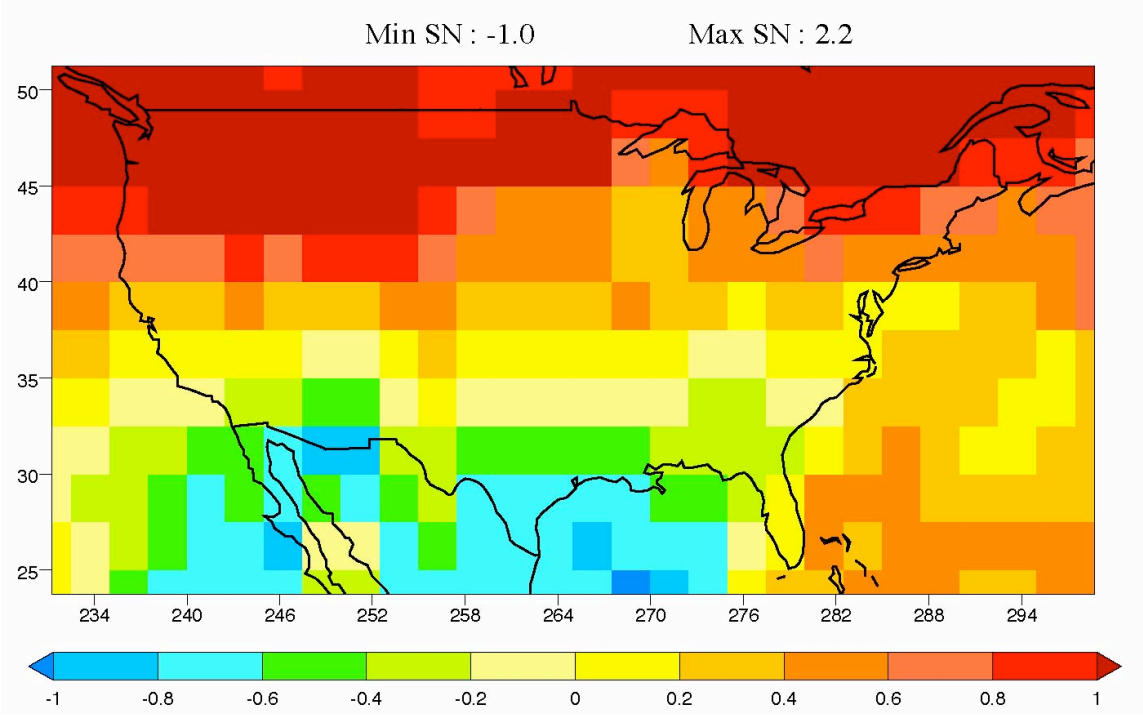

Fig 10a: Ratio of the all-model mean DJF precipitation response (to doubled atmospheric CO_2 concentration) to the standard deviation of the response over the 15 models

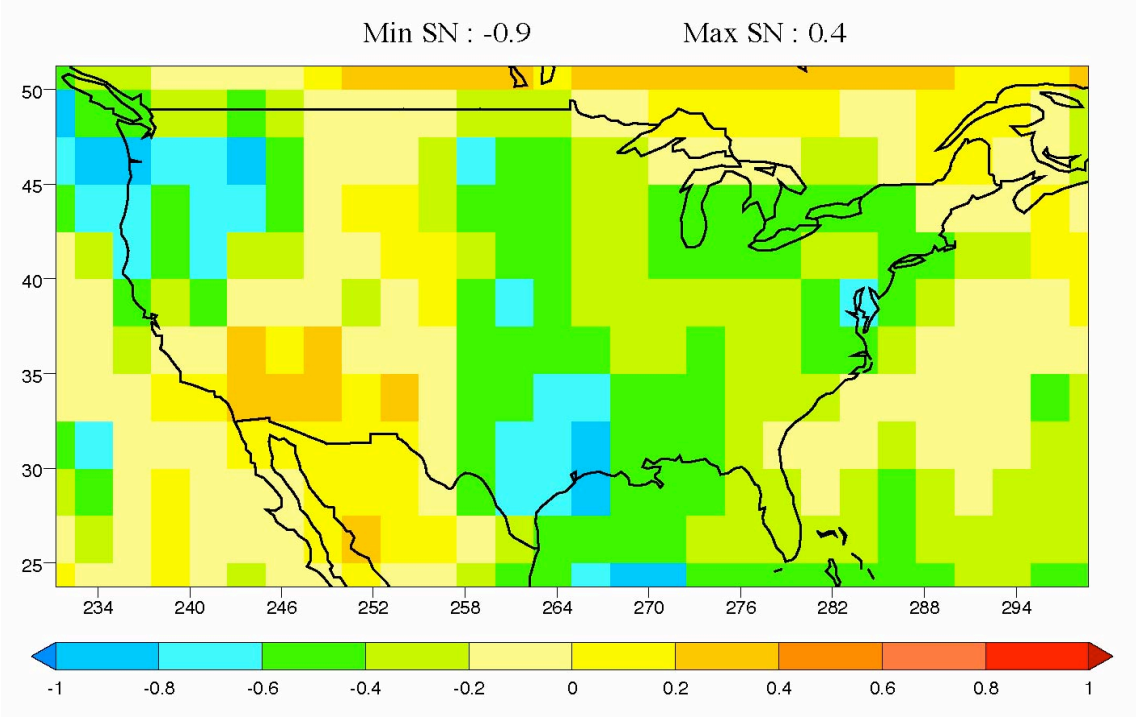

Fig 10b: Same as Fig 10a, for the JJA precipitation response.

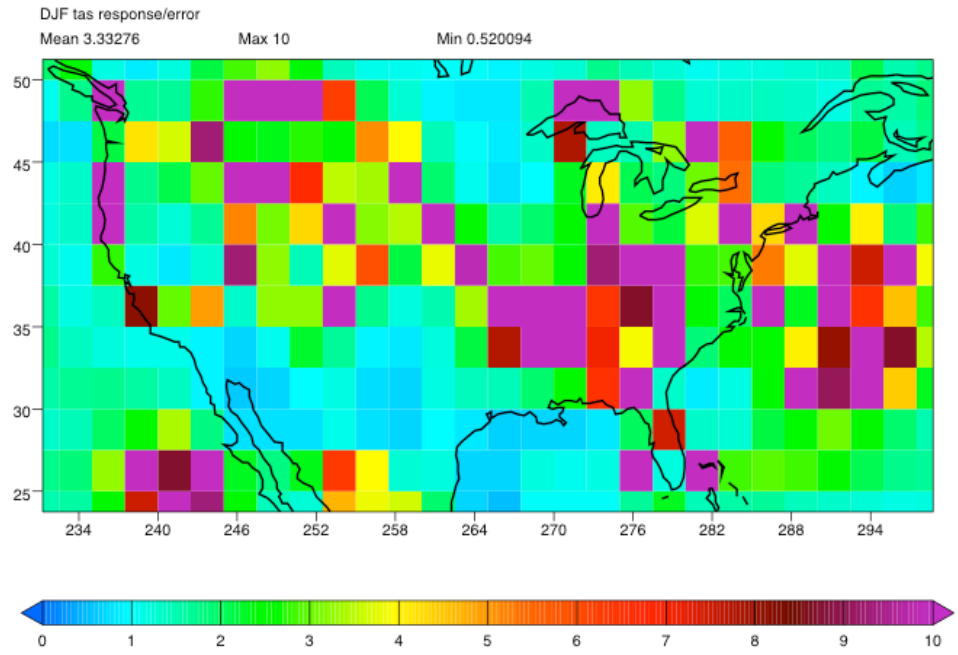

Fig. 11a: All-model mean response in near-surface temperature to increased C02, divided by error in all-model mean near-surface temperature, for DJF.

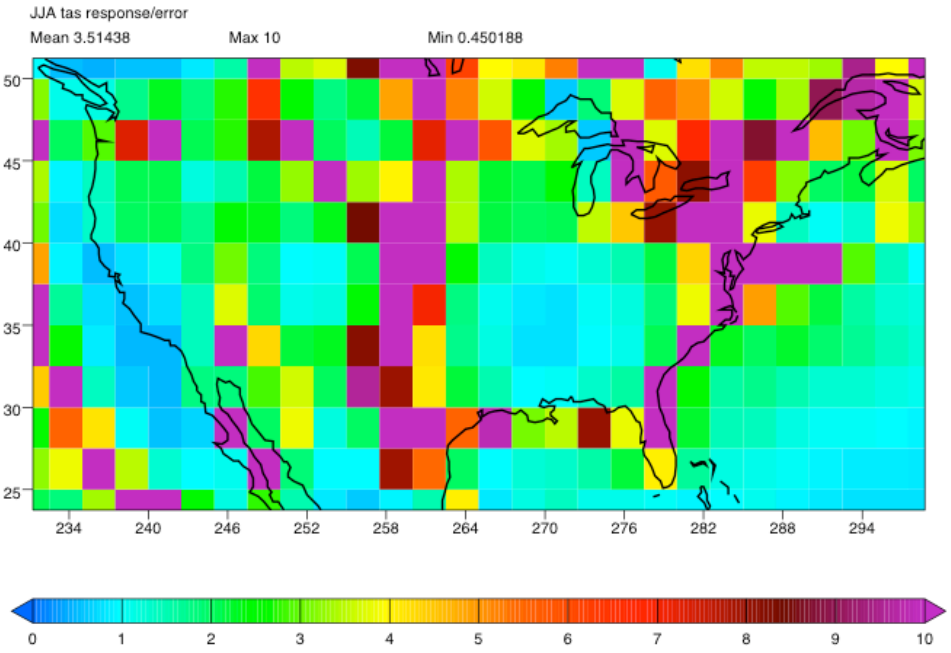

Fig. 11b: Same as Fig. 11a, for JJA.

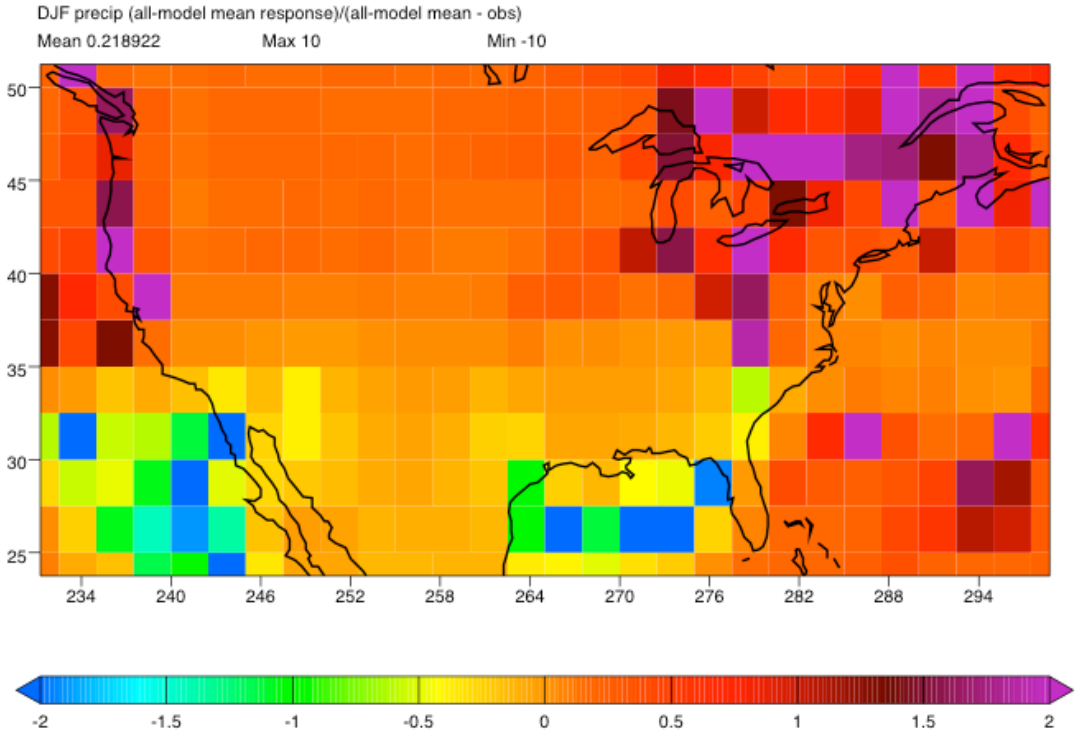

Fig. 11c: All-model mean response in precipitation to increased CO_2, divided by error in all-model mean precipitation, for DJF.

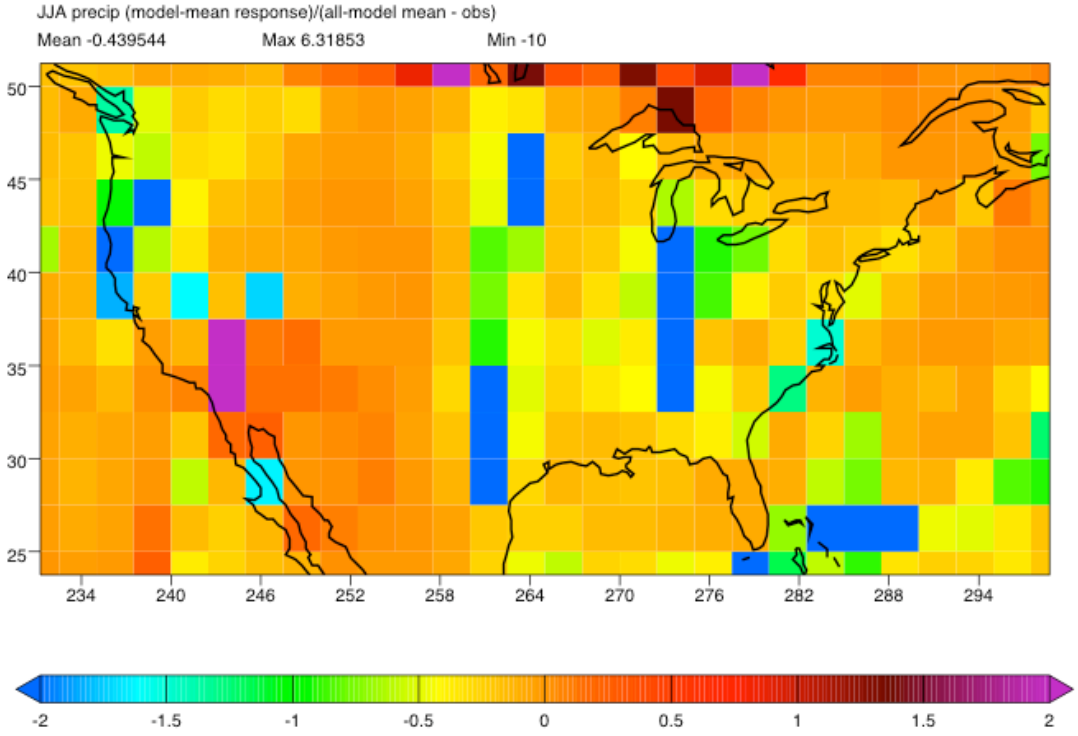

Fig. 11d: Same as Fig. 11c, only for JJA

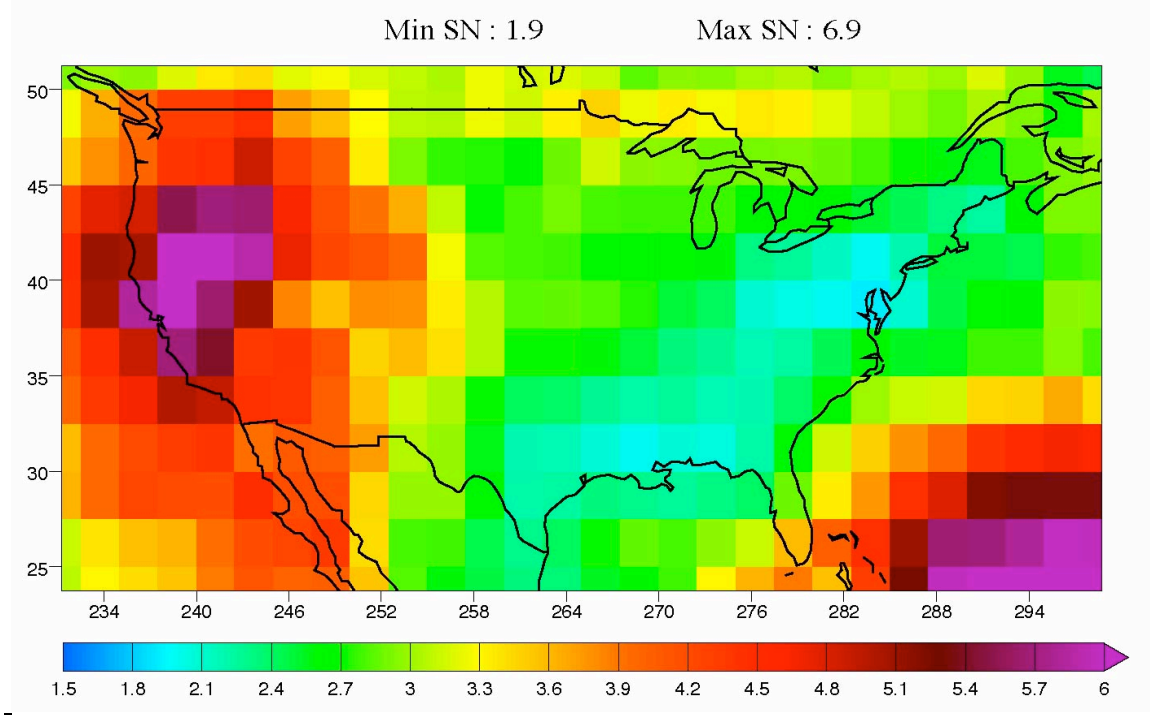

Fig 12: Same as Fig 10, for the DJF near-surface temperature response

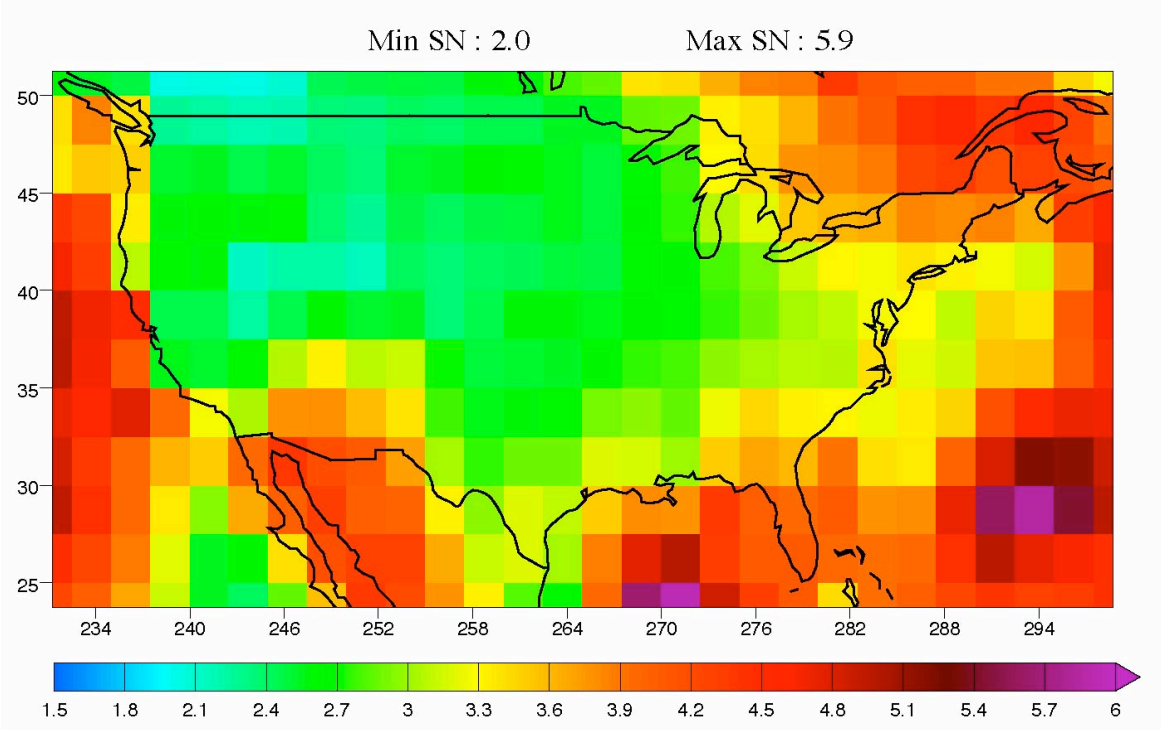

Fig 13: Same as Fig 10, for the JJA near-surface temperature response.

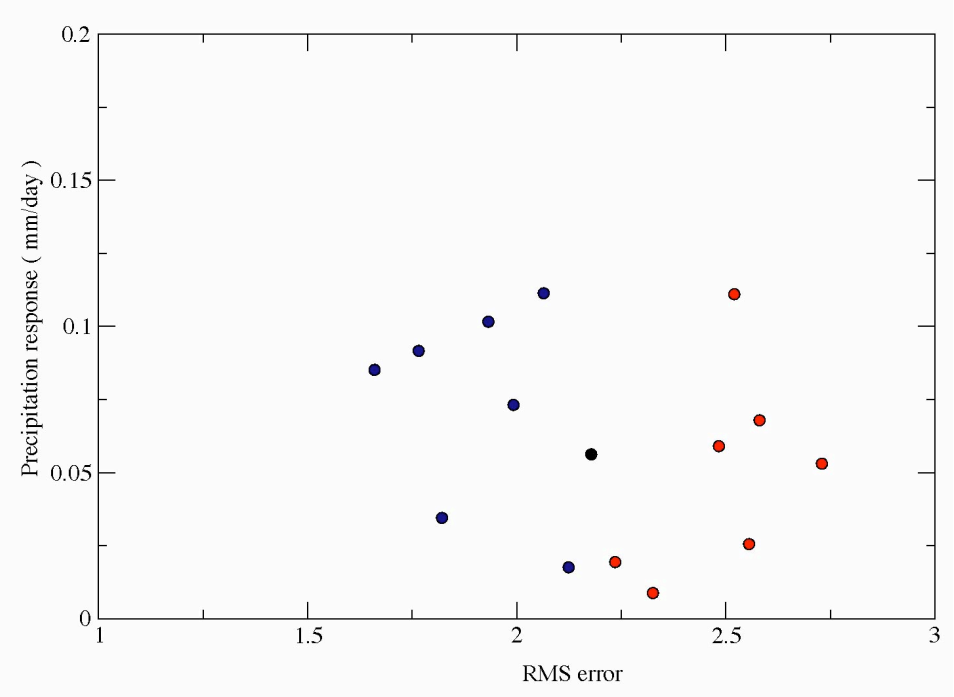

Fig. 14: Annual mean precipitation response to doubled CO_2 atmospheric concentration, over latitudes 60S to 60N versus RMS error calculated over the same region, over each month of the year.

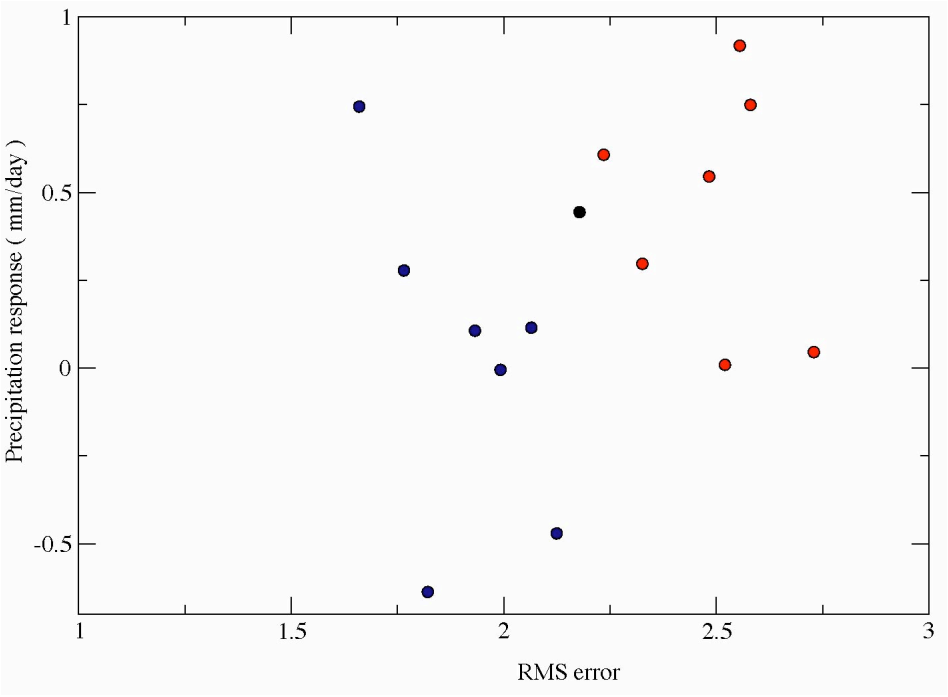

Fig. 15: Precipitation response to doubled CO_2 atmospheric concentration, over the western U.S. in DJF versus RMS error calculated over latitudes 60S to 60N, over each month of the year

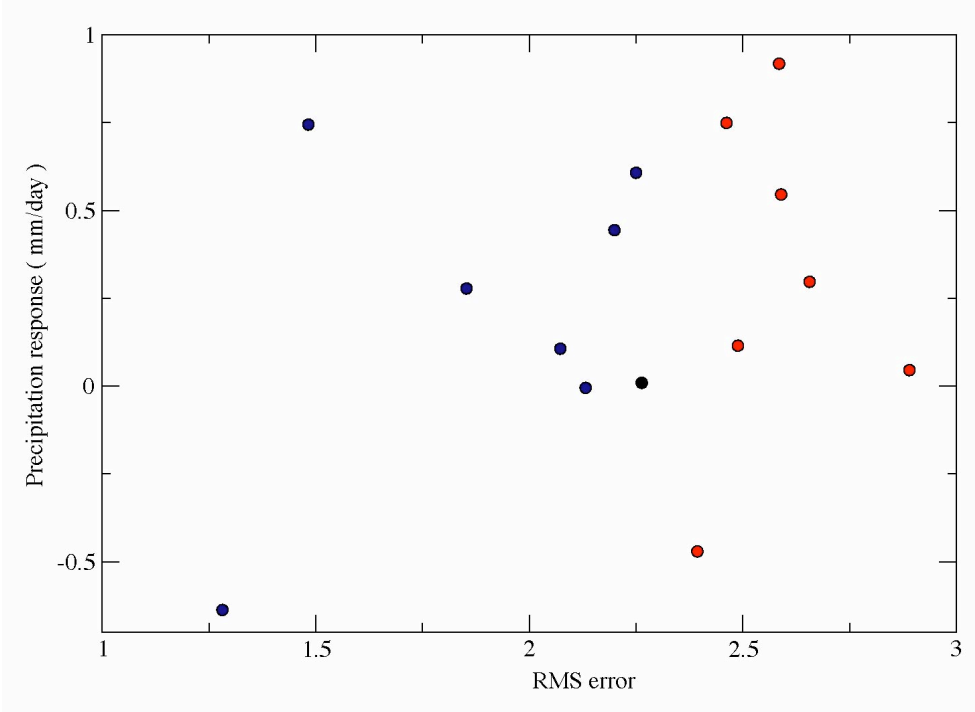

Fig. 16: Precipitation response to doubled CO_2 atmospheric concentration, over the western U.S. in DJF versus RMS error calculated over the North-Eastern Pacific region, over each month of the year

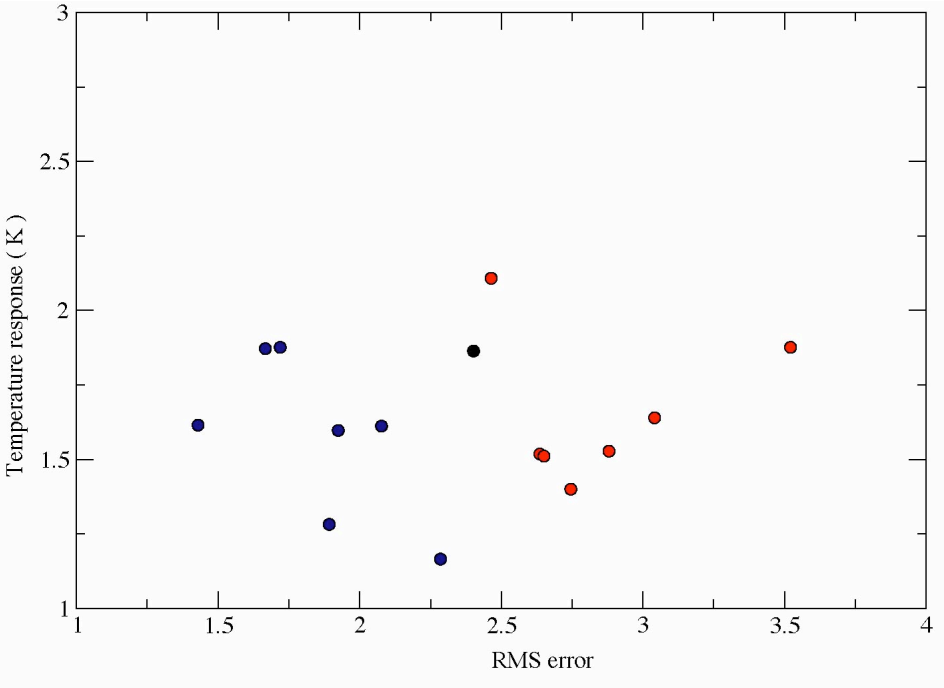

Fig. 17: Annual mean temperature response to doubled CO_2 atmospheric concentration, over latitudes 60S to 60N versus RMS error calculated over the same region, over each month of the year

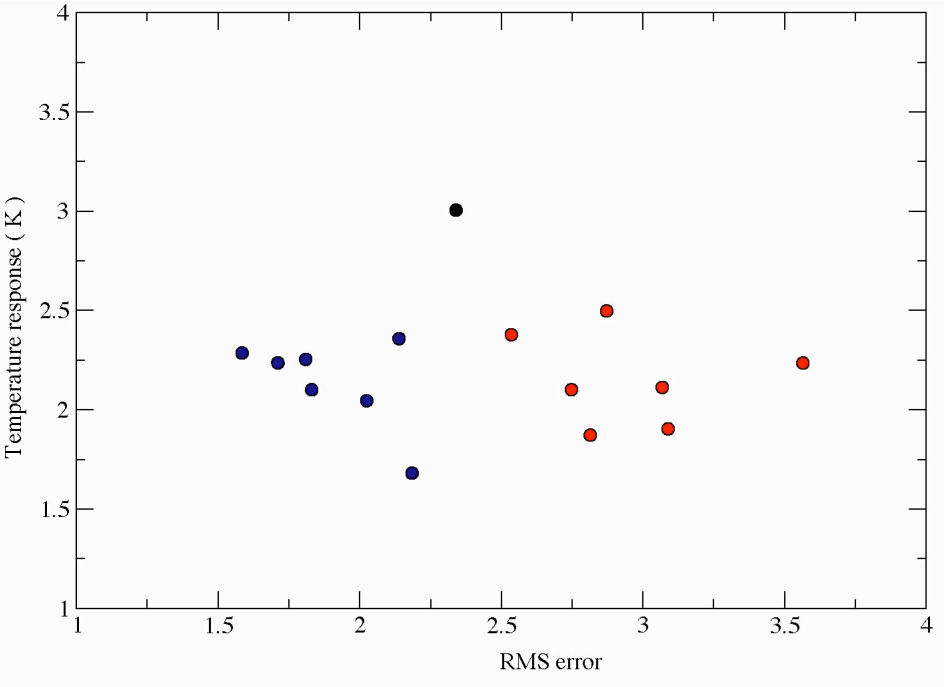

Fig. 18: Temperature response to doubled CO_2 atmospheric concentration, over the western U.S. in DJF versus RMS error calculated over latitudes 60S to 60N, over each month of the year

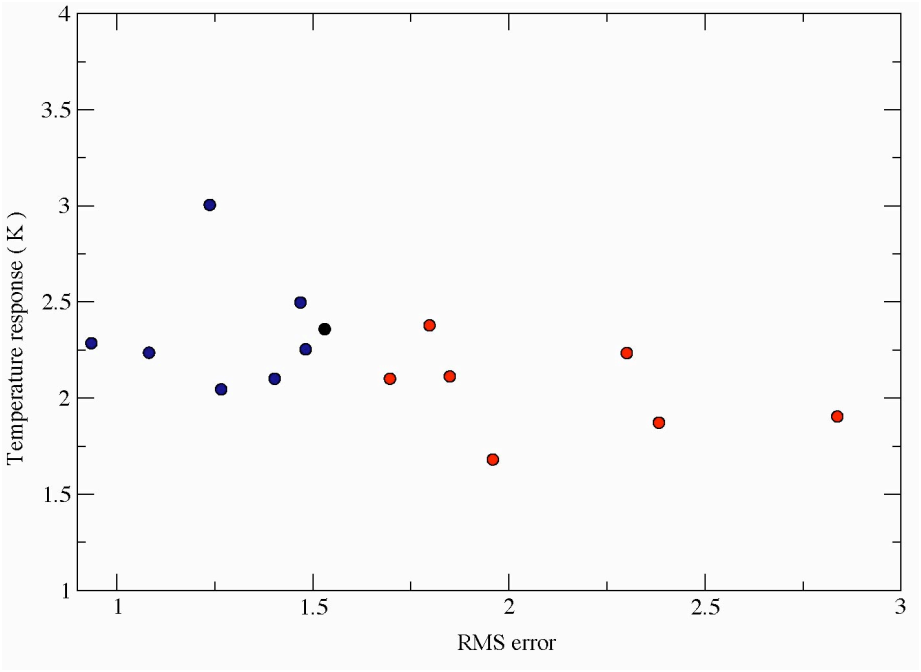

Fig. 19: Temperature response to doubled CO_2 atmospheric concentration, over the western U.S. in DJF versus RMS error calculated over the North-Eastern Pacific region, over each month of the year

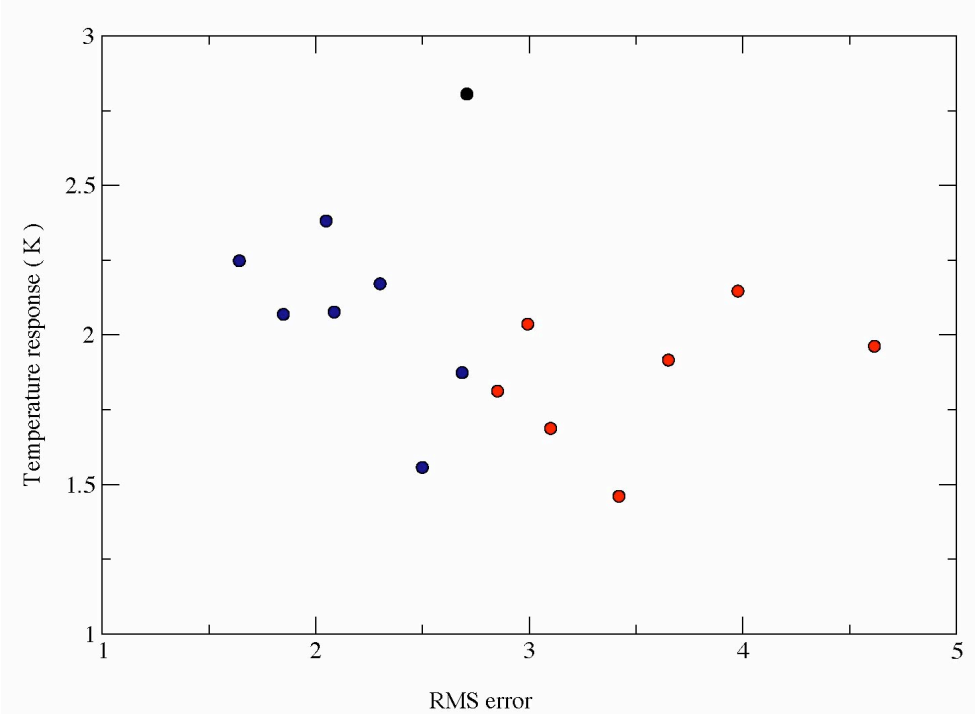

Fig. 20: Temperature response to doubled CO_2 atmospheric concentration, over Europe in DJF versus RMS error calculated over the Northern Atlantic region, over each month of the year

University of California
Lawrence Livermore National Laboratory
Technical Information Department
Livermore, CA 94551